VYSOKÉ UČENÍ TECHNICKÉ V BRNĚ
BRNO UNIVERSITY OF TECHNOLOGY

FAKULTA STROJNÍHO INŽENÝRSTVÍ
FACULTY OF MECHANICAL ENGINEERING

ENERGETICKÝ ÚSTAV
ENERGY INSTITUTE

IN VITRO STUDY OF THE EFFECT OF PARTICLE CHARACTERISTICS AND FLOW RATE ON REGIONAL DEPOSITION IN HUMAN AIRWAYS

IN VITRO IN VITRO VÝZKUM VLIVU VLASTNOSTÍ ČÁSTIC A PRŮTOKU VZDUCHU NA REGIONÁLNÍ DEPOZICI V DÝCHACÍCH CESTÁCH ČLOVĚKA STUDY OF THE EFFECT OF PARTICLE CHARACTERISTICS AND FLOW RATE ON REGIONAL DEPOSITION IN HUMAN AIRWAYS

TEZE
SHORTENED VERSION OF PhD THESIS

AUTOR PRÁCE
AUTHOR

Ing. Miloslav Bělka

ŠKOLITEL
SUPERVISOR

doc. Ing. Jan Jedelský, Ph.D.

BRNO 2018

Keywords

Particle deposition, aerosol transport, porous particles, fibers, replica of respiratory airways

Klíčová slova

Usazování částic, transport částic, porézní částice, vlákna, model dýchacích cest

Místo uložení práce

Oddělení pro vědu a výzkum FSI VUT v Brně

Contents

1. Introduction

The human respiratory system is a gateway to our body. When we breathe in ambient air, we can bring air pollutants into our lungs and subsequently into our system. Air pollution exposure contributes to increase rates of asthma or worsening of existing respiratory diseases, such as chronic obstructive pulmonary disease (COPD) or lung cancer (Laumbach and Kipen, 2012). The mortality from chronic respiratory diseases is estimated to be 4 million people worldwide annually (FIRS, 2013). Moreover, inhaled nanoparticles can also translocate to other organs via bloodstream and cause additional harm (Oberdorster et al., 2004). Of course, air pollution is not the only trigger for respiratory diseases, e.g. COPD is mainly caused by cigarette smoking (Burney et al., 2015). Generally, understanding the particle transport and subsequent deposition in the respiratory tract is the first step to estimate the particle´s health hazards.

The study of particle deposition is also motivated by inhalation medicine. As inhalation of airborne particulate matter can trigger or exacerbate respiratory diseases, inhalation of aerosolized medicaments is frequently used for treatment of respiratory diseases, such as asthma or COPD. Moreover, inhalation therapy can also provide a systemic drug delivery of various therapeutic peptides and proteins as the respiratory tract is richly supplied with blood (Agu et al., 2001).

To efficiently utilize the potential of inhalation therapy or to sufficiently estimate health hazards of particulate matter, it is essential to comprehend the particle transport and subsequent deposition. Particle transport through the respiratory tract is affected mainly by breathing pattern, lung geometry and particle characteristics. The effect of various factors on deposition needs to be emphasized. Moreover, the deposition distribution is not uniform throughout the airways and therefore, study of localized deposition is of great concern. As the deposition patterns of spherical particles have been thoroughly investigated, the aim of this thesis is to analyze the effect of particle non–spherical shape and inhalation flow rate on deposition.

1. State of the art

The particle deposition in human respiratory system can be studied using three approaches: *in vivo, in vitro* and *in silico*. *In vivo* methods employ human subjects in the measurements. *In vitro* methods utilized various dummy models to simulate conditions in real organisms. *In silico* methods use mathematical models or numerical simulations to predict particle transport and deposition. All the methods have their advantages and drawbacks and the choice depends on the information wanted. The studies can obtain information about total or regional deposition. Total deposition adds up particle deposition in all regions of the respiratory airways. Regional deposition provides more detailed information about the effective dose in various regions of the lungs, such as lung lobes or airway generations.

1.1. *In vivo* methods

Total deposition can be easily obtained by *in vivo* measurements by comparing particle concentration of inhaled and exhaled air using various photometers. Well-controlled (prescribed breathing pattern and flow rate) inhalation of monodisperse particles results in considerably good deposition prediction related to particle size and breathing pattern. Total deposition studies have been performed for decades (Foord et al., 1978; Heyder et al., 1975; Schiller-Scotland et al., 1994; Stahlhofen et al., 1989). For example, Heyder et al. (1975) studied total deposition of particles in the range from 0.1 to 3.2 μm while breathing by nose or mouth. Later on, Heyder et al. (1986) experimentally determined total deposition of particles in the range 0.005–15 μm.

The ratio of total particles inhaled and exhaled can be also utilized in the measurements of regional deposition using an aerosol "bolus" technique. The bolus technique can be traced back to Alshuler (1969) who described its potential in aerosol dispersion or estimating regional deposition. During this procedure, a subject breathes at regular intervals and a small bolus of particles is introduced at a predetermined point of inspiration. The point of inspiration determines how deeply the bolus penetrates the respiratory system. The depth that is reached by a bolus is usually referred as the penetration volume (V_p) and is defined as the volume of air inhaled from the mode of the bolus to the end of inspiration (Darquenne, 2012). By delivering boluses at different points of inspiration and comparing the fractional depositions, regional deposition in various parts of the respiratory system is estimated. The first applications of this technique were reported by Muir et al. (1970). Heyder et a. (Heyder et al., 1988) employed this technique to study convective mixing in the respiratory airways. The bolus was inspired to different depths of the airways and the extent to which the aerosol spread was measured. Kim et al. (1996) assessed regional deposition in healthy nonsmoking men. Boluses of monodisperse particles (1, 3, and 5μm) were delivered to various lung depths (V_p ranged from 100 to 500 mL) in 50 mL increments and three flow rates. Representative data of deposition fraction in local volumetric regions are shown in Figure 9.

Another approach how to assess regional deposition of inhaled particles *in vivo* can be a use of radionuclide imaging methods. These methods label particles with various radionuclides. Subject inhales the particles and images of lungs by one or multiple gamma cameras are taken afterwards. The advantage of this imaging is the actual picture of particle deposition in human lungs. The drawbacks include the high cost, high radiation doses and complexity of the methods. The use of these techniques is predominantly in inhalation medicine to study where the particles deposit and how quickly they are removed, i.e. lung clearance.

.

1.2. *In vitro* methods

Aerosol regional deposition can be measured by *in vitro* methods using physical airway casts. The deposition studies using these casts can simulate realistic inhalation and deposition airway by airway can

be examined. Moreover, deposition experiments can be reproduced. A series of experiments can be performed to study the effect of particle size or breathing regime on deposition under the same conditions. On the other hand, neither the available morphological data nor the technology allow production of the complete realistic lung cast. Therefore, regional deposition only in the upper respiratory tract and large airways of the tracheobronchial tree can be assessed.

The airway models have either idealized or realistic geometry. The idealized geometries were constructed with critical dimensions corresponding to available measured data of human respiratory tract or chosen aerodynamic principles (Byron et al., 2010). The casts encompass single or multiple cylindrical bifurcations made of plastic, glass, metal etc. The dimensions often correspond with dichotomous lung model of Weibel (1963). The realistic geometries are based either on casts from dental negatives and cadavers (Cheng et al., 1997) or on CT and MRI scans (Grgic et al., 2004; Lizal et al., 2012; Tian et al., 2017).

1.3. *In silico* methods

The most significant drawback of the experimental *in vivo* data is in the limited number of tested subjects, selected breathing patterns and particle sizes. This data gap is often filled with *in silico* methods. *In silico* modelling concepts may be grouped according to the region of interest in the lung, i.e. prediction of deposition in the whole lungs (respiratory system) or prediction of deposition in selected small regions, such as airway generation, using Computational fluid dynamics approach (CFD) (Hofmann, 2011).

The whole lung approach simplifies the phenomena and treats the airflow, particle transport and deposition independently. The particle deposition is described by analytical deposition equations for various flow conditions. The whole lung models may be divided into five groups: empirical and semi–empirical, mechanistic 1D, deterministic symmetric, deterministic multi–path, and stochastic models (Hofmann, 2011; Rostami, 2009).

CFD methods are the most recent mathematical techniques used for the study of regional deposition. Unlike whole lung models that use 1D analytical equations, CFD methods use 3D general governing transport equations for the fluid flow analysis. The fluid flow is determined by solving Navier-Stokes equations which describe the relationship of velocity, pressure, temperature, density and viscosity (Versteeg and Malalasekera, 2007). The particle deposition is then calculated using Lagrangian or Eulerian approach. The former approach tracks individual particles through the computational geometry by solving Newton´s second law equation (Longest and Xi, 2007). The second approach considers particles as a continuum phase and solves transport equations for aerosol concentration. The Eulerian approach is more appropriate for high concentrations and ultrafine particles for which inertia is negligible (Rostami, 2009).

During the CFD process, the airway geometry is divided into small representative elements and detailed solution of fluid flow and particle transport is calculated in each element afterwards. As the elements can have sub-millimeter sizes, CFD can provide very localized deposition patterns that are not possible to obtain by other approaches. However, the higher number of representative elements (the size and complexity of the geometry) results in higher computational times. Therefore, the CFD methods are currently employed to elucidate flow and deposition patterns in separated airway sections, such as an oral cavity, an airway bifurcation etc. The CFD model of the whole lung is not yet feasible. However, the size of the computed regions increases with increasing computational power (Longest and Holbrook, 2012).

The CFD methods are used to analyze deposition in extrathoracic airways, upper tracheobronchial tree or alveolar region. The geometries are similar to those used in the airway cast studies. Using the same geometry for both *in vitro* and *in silico* CFD approaches is convenient as the results can be easily compared. This is important because the underlying physics used in CFD methods is very intricate and the results need to be validated by experimental evidence (*in vitro* or *in vivo*).

The CFD methods have been frequently used for aerosol deposition studies. Various idealized (Zhang et al., 2004) or realistic geometries (Lambert et al., 2011) were employed. Several reviews (Cheng, 2014; Kleinstreuer et al., 2008; Longest and Holbrook, 2012; Rostami, 2009) have been published regarding this topic.

1.4. Special cases affecting particle transport and deposition

The particle transport and subsequent deposition is generally affected by several factors, e.g. respiratory tract geometry, breathing pattern and particle characteristics (Kleinstreuer and Feng, 2013). Deposition of particles under normal conditions, i.e. deposition of spherical particles in human adult lungs under various breathing regimes, has been widely studied and can be accurately predicted by various *in vivo* or *in silico* methods. However, special cases, such as deposition of non-spherical particles in diseased or infant lungs has not been fully understood. Some of the examples will be discussed here.

a) Analysis of fiber deposition

Although most studies were performed using spherical particles, naturally occurring particles usually have non-spherical shapes. Fibrous particles are of great interest because exposure to fibrous particles may result in various health problems. For example, exposure to asbestos fibers can lead to onset of asbestosis or lung cancer (Su and Cheng, 2009).

Fiber aerodynamic behavior is different than that of spherical particles. Fibers tend to align with its main axis parallel to the air flow direction causing their effective aerodynamic diameter to closely approximate fiber diameter (Baron, 2001). Because of this phenomenon, fibers react to changes of flow direction more easily compared to spherical particles and their deposition patterns are different. During fiber motion through the respiratory airways, fibers occasionally rotate. The frequency of rotation depends on the fiber aspect ratio and local velocity gradients (Feng and Kleinstreuer, 2013). Since the fibers are hazardous to human health, experiments using human volunteers are unethical and strictly forbidden. Therefore, the total and regional deposition of fibrous aerosol have been analyzed only via *in vitro* and *in silico* approaches.

The number of experimental studies on fiber deposition to date is rather sparse. One of the obstacles during *in vitro* experiments is a complicated generation of monodisperse fiber aerosol. Therefore, polydisperse fibers have been usually employed during the experiments and the deposition of fibers having specific diameter or length was determined by means of optical or electron microscopy afterwards. Myojo (1987) and Myojo (1990) studied deposition of polydisperse glass fibers in the bifurcation model at several steady inhalation flow conditions. The fibers deposited mostly around bifurcation ridges and the deposition fraction increased with increasing flow rate and dimensions. Sussman et al. (1991) examined deposition of crocidolite fibers in a realistic cast of tracheobronchial tree made from cadaver. The fibers were aerodynamically classified having diameters from 1.5 to 2.5 μm and various lengths. It was observed that both the length and flow rate affected deposition. Comprehensive study of fiber deposition in two realistic airway casts was presented by Su and Cheng (2005, 2006, 2009) and Zhou et al. (2007). Regional deposition of various fiber types, such as carbon or glass, was examined by optical microscopy. Deposition hot spots were found in the oropharynx and around bifurcation ridges (Figure 1). The deposition fractions increased with increasing flow rate and dimensions (diameter and length) and was represented by a single parameter, Stokes number for randomly oriented fibers. Later, Su and Cheng (2015) investigated deposition of size classified fiber nanotubes in the same airway cast.

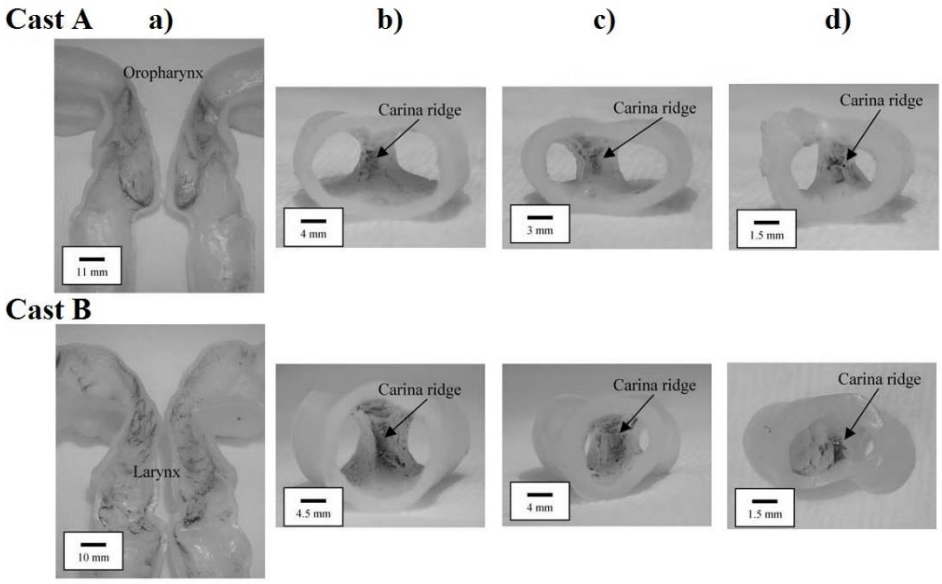

Figure 1 The deposition hot spots in the two realistic airway casts for steady inhalation of 43.5 L/min: a) oral cavity and throat, b) 1st bifurcation, c) 2nd bifurcation, c) 3rd bifurcation (Su and Cheng, 2006)

When studying regional and total fiber deposition using *in silico* methods, one needs to mathematically describe a complex fiber movement, both translation and rotation, in the fluid flow and take into account several deposition mechanisms including interception. Many theoretical (Asgharian and Yu, 1989; Harris and Fraser, 1976; Jeffery, 1922) or empirical models (Myojo and Takaya, 2001) for deposition estimations have been presented in the past. These models were incorporated into Euler equations to describe fiber transport and orientation (Asgharian and Anjilvel, 1995a; Fan and Ahmadi, 1995).

With the increase in computational power, the derived equations got employed in numerical analysis of fiber deposition in the respiratory airways. Zhang et al. (1996) numerically calculated fiber deposition in equal-diameter bifurcation model. Equations for fiber trajectories given by Asgharian and Anjilvel (1995b) together with the Navier-Stokes equations were solved. The majority of fibers deposited around the bifurcation ridge via impaction and interception. Shanley and Ahmadi (2011) implemented the same equations into a CFD solver and studied fiber transport and deposition in a horizontal pipe. The empirical expressions were proposed to predict fiber sedimentation rates under various flow conditions. Later, Shanley et al. (2016) analyzed fiber transport and deposition in a realistic model of the nasal airways. Tian et al. (2012) employed the numerical model of Fan and Ahmadi (1995) and studied fiber transport in low Reynolds number flows using computational modelling. Later, Tian and Ahmadi (2013) investigated fiber transport and deposition in a multiple bifurcation model. The study showed that fibers travelled aligned with the main air flow stream and occasionally exhibited impulsive rotation behavior that enhanced deposition by interception. The fibers deposited by impaction around bifurcation ridges mainly in the 1st bifurcation (Figure 2). Moreover, the fiber aspect ratio enhanced deposition indicating significant role of inertia. Feng and Kleinstreuer (2013) studied fiber deposition in a realistic human respiratory model encompassing respiratory airways from mouth to the 4th generation of bronchial branching. Inthavong et al. (2013) investigated carbon and glass fiber deposition in the realistic model extending from the nasal cavity to the main bronchi (Figure 3). Instead of solving equations describing fiber transport and orientation, an empirically defined drag coefficient was applied to account for the random fiber behavior.

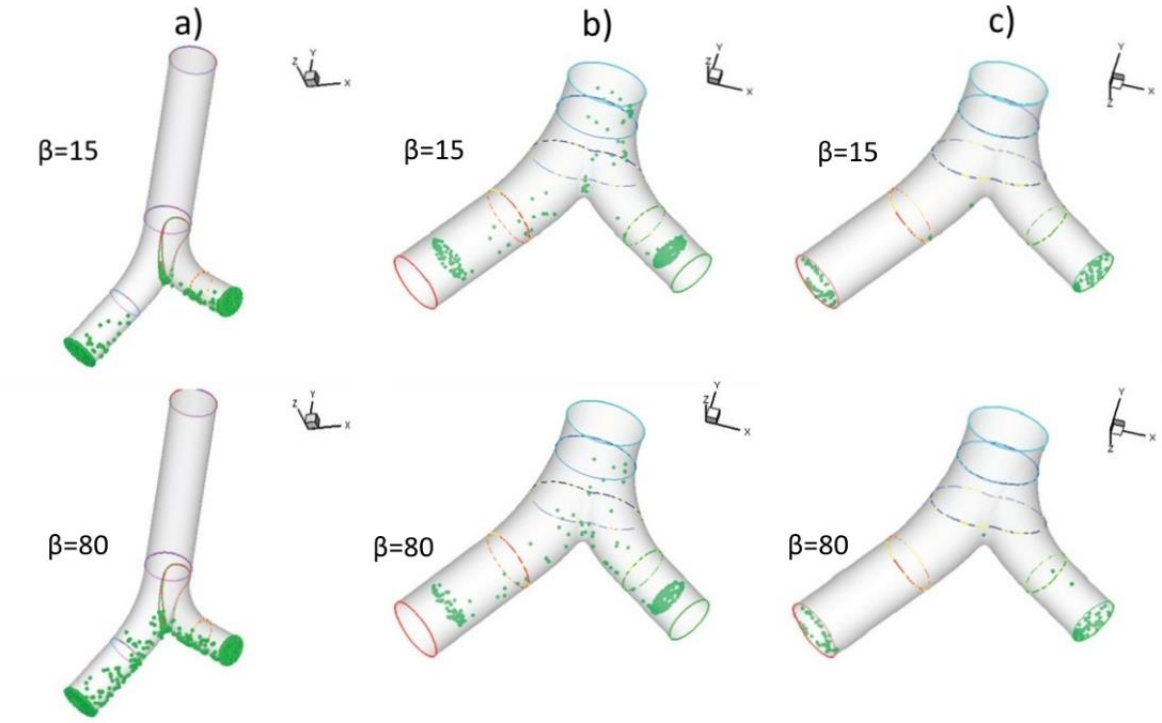

Figure 2 Deposition patterns of carbon fibers (d = 3.66 μm) with various aspect ratios in the first three bifurcation of the tracheobronchial tree under the flow rate of 40 L/min; a) trachea and 1st bifurcation, b) 2nd bifurcation, c) 3rd bifurcation (Tian and Ahmadi, 2013)

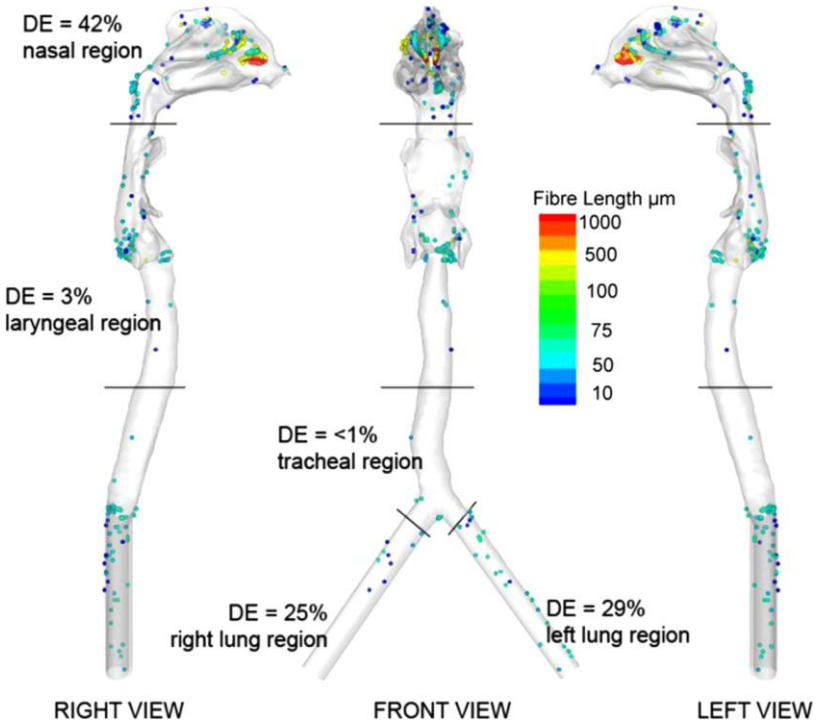

Figure 3 Deposition patterns of carbon fibers under the flow rate of 15 L/min (Inthavong et al., 2013)

b) Analysis of porous particle deposition

Presence and deposition of particles in the respiratory tract does not always result in possible health hazards. The respiratory route is also frequently used for delivery of aerosolized medicaments. Inhalation of the medicine is commonly utilized for treatment of respiratory diseases, such as chronic obstruction pulmonary disease (COPD). However, it can also provide a systemic drug delivery of various therapeutic peptides and proteins via air-blood barrier (Pirozynski and Sosnowski, 2016).

For systemic drug delivery, a penetration into respiratory zone of the lungs is necessary and therefore, the optimum aerodynamic size of particles ranges between 1 and 3 μm (Edwards et al., 1997). Following the basic aerodynamic concept, the optimum size can be achieved by unit density particles in the range of 1–3 μm or by larger particles with lower density. Nowadays, large porous particles are a very promising platform. They are characterized by large size (> 5 μm, up to 30 μm) and low density (usually < 0.4 g/cm^3) (Gharse and Fiegel, 2016).

Porous particles can be formulated by various methods, such as spray drying, spray freeze drying, crystallization, supercritical fluid technologies etc. The spray drying method is the most frequent for porous particle production as this method produces particles of relatively uniform size and shape. The review of the methods can be found elsewhere (Gradon and Sosnowski, 2014; Shoyele and Cawthome, 2006).

The porous particles are formulated for medical purposes and, as other forms of aerosolized medicine, they are administered via inhalers. The assessment of drug delivery systems is performed following U.S or European Pharmacopeias instructions (Mitchell and Nagel, 2003). These instructions recommend a use of cascade impactor to measure an aerodynamic particle size distribution and mass median aerodynamic diameter (MMAD). Limited information about deposition is then based on the given particle size distribution. Fine particle fraction (FPF) is determined as having the mass median aerodynamic diameter less than 5 μm (Council of Europe, 2007) and it is assumed that the FPF penetrates the upper respiratory airways and reaches the lungs. Many studies concerning porous particles have employed this procedure to assess the fate of the particles in the lungs (Dellamary et al., 2000; Gervelas et al., 2007; Nolan et al., 2009; Vanbever et al., 1999). However, these attempts to connect aerodynamic particle size distributions and respiratory tract deposition are not adequate as the deposition is affected by many other factors than only particle size (Mitchell et al., 2007).

Other methods, such as *in vivo* or *in silico*, have been employed to provide more realistic and more detailed information about regional deposition of porous particles. In some of the studies, the aerodynamic particle size distribution measured by a cascade impactor was utilized as an input parameter into the whole-lung deposition models. For example, Dunbar et al. (2002) measured sizes of large porous particle placebo formulations (MMAD of 3 and 5 μm) using multistage liquid impinger. The extrathoracic and lung deposition was then calculated using the ICRP model. The percentage of 3 μm and 5 μm particles that would reach the lungs was estimated as 60% and 45%, respectively. Musante et al. (2002) employed a developed mathematical model and predicted deposition of large porous particles and aerodynamically similar but geometrically smaller particles. The results indicated that small submicron particles had higher deposition efficiency in the lower respiratory airways compared to porous particles because of the effect of diffusion. Other studies have employed *in vivo* methods, in particular a gamma scintigraphy method. Hirst et al. (2002) investigated deposition of Pulmosphere^{TM} porous particles and conventional micronized particles in nine nonsmoking subjects. It was found out that the oropharyngeal deposition fraction of porous particles was lower compared to conventional particles (42.6±9% vs. 72±8%) and the total lung deposition was approximately double in the case of porous particles (28.5±11.3% vs 14.5±8.1%). However, the information about particle agglomeration was not obtained and therefore, it is complicated to evaluate the effect of shape on deposition. Dunbar et al. (2002) obtained regional deposition of 3 and 5 μm porous particles in several healthy subjects. The lung deposition for 3 and 5 μm particles was 59% and 37.3% on average, respectively. The *in vivo* results were compared to those obtained by a cascade impactor in combination with ICRP model. It was concluded that the ICRP model overpredicted the deposition for larger particles and the intersubject variability was not captured by the ICRP model.

2. Aims of the thesis

The study of particle deposition is very complex and highly investigated topic. Generally, the *in vivo* methods and the "whole-lung" *in silico* models are frequently used to predict deposition of spherical particles during normal conditions in the entire respiratory system. The use of CFD methods in conjunction with *in vitro* methods can be utilized for special cases, such as non–spherical particles, or to predict localized deposition in specific parts of the respiratory tract.

The aim of this research is to study the effect of particle shape and inspiratory conditions on regional deposition in the replica of human respiratory airways that was developed at our department. The deposition data may be used to elucidate the complicated transport mechanisms of non-spherical particles, such as fibers. Moreover, experimental data are crucial for validation of CFD methods, which have become a convenient tool for study of particle transport and deposition in human respiratory airways. The objectives of this research were determined at the state doctoral examination and are listed below:

- Analysis of porous particle deposition.
    - Generation of porous particles.
    - Choice of proper method for deposition detection.
    - Carrying out of deposition experiments.
    - Analysis of the results.

- Analysis of fiber deposition
    - Generation of monodisperse fiber aerosol.
    - Choice of proper method for deposition detection.
    - Carrying out of deposition experiments.
    - Analysis of the results.

2.1. Scientific question

How is the deposition efficiency or fraction of non–spherical particles related to that of spherical particles?

2.2. Hypotheses

- *It is expected that the deposition efficiency of porous particles throughout the respiratory airways is similar to that of spherical particles having the same aerodynamic diameter*
- *It is expected that fibers deposit less effectively than spherical particles having the same aerodynamic diameter*

3. Results

3.1. Objective 1 - Deposition of porous particles

The objective was to determine a deposition of porous particles. To do this, porous particles of suitable size and density had to be produced. The produced porous particles were supposed to be introduced into the replica and deposit there. Proper detection method had to be found to quantify the regional particle deposition.

a) Porous particle generation

Several methods, such as spray–freeze drying, spray drying, liquid–liquid interfacial crystallization, were tested to produce particles with porous structure. A market screening was performed to obtain porous particles with suitable properties. All the particles were analyzed in the terms of density and size and the results can be found in Table 1.

The spray–freeze drying method and crystallization of NaCl produced particles that were large with diameters in the order of tens of micrometers. As the maximum recommended particle size is 30 μm, these particles were not suitable for the use in deposition experiments. In the case of spray–freeze drying there was a problem with agglomeration. The particles agglomerated during particle spraying and the proper solution for particle deagglomeration was not found. On the other hand, the density of the particles produced by the spray–freeze drying method was the lowest from all the produced particles. The crystallization of the NaCl also produced low density particles and it was indicated that the porosity of the particles increased with decreasing molar concentration.

The particles produced by spray drying method or crystallization of $CuSO_4 \cdot 5H_2O$ had suitable sizes ($d_p < 30$ μm). The aerodynamic size distribution of these particles can be seen in Figure 4 together with size distribution of commercially obtained particles (the silica particles). Relative counts were used for an easy comparison. The narrowest size distribution had silica particles. Spray drying method produced particles with narrower size distribution (lower standard deviation) compared to the crystallization method. Comparing the mass median aerodynamic diameters, the MMAD of particles produced by crystallization method was rather high indicating that significant number of large particles was produced by this method. The bulk density of $CuSO_4$ particles only slightly exceeded the recommended value of 0.4 g/cm^3. The density of the chitosan particles produced by spray–drying method was not determined as the process was not optimized at the time and the output volume was too low.

The most suitable particles in the terms of sizes and density were silica particles. However, given the financial sources it would not be possible to obtain enough particles for deposition experiments. The spray drying method produced particles with narrowest size distribution which is needed for deposition experiments. However, the output was too low. That is why the $CuSO_4$ particles were chosen to be used in the deposition experiments.

Table 1 Characteristics of the produced porous particles

Particle type	Particle size (μm)	Tapped density (g/cm^3)	Bulk density (g/cm^3)
Freeze–spray drying (chitosan)	Equivalent diameter of 21.2±23.4	0.11	0.09
Spray drying (chitosan)	CMAD of 3.5±1.8 MMAD of 5.9±1.6	–	–
Crystallization (NaCl)	–	0.48	0.37
Crystallization ($CuSO_4 \cdot 5H_2O$)	CMAD of 1.9±1.9 MMAD of 7.4±1.7	0.54	0.42
Silica porous particles	CMAD of 4.1±2.2 MMAD of 4.7±1.3	–	0.45

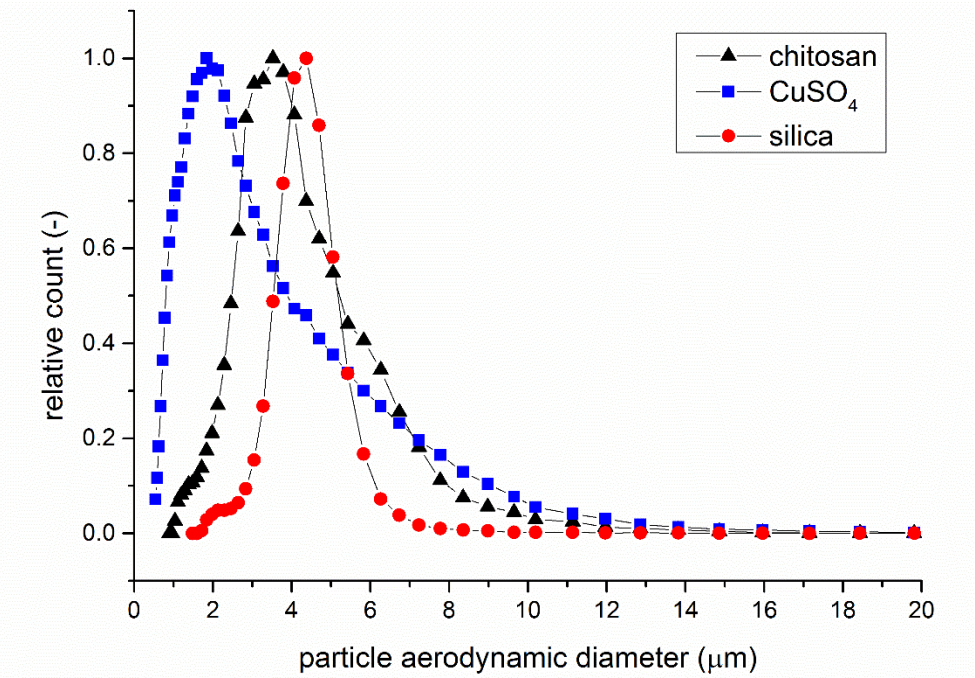

Figure 4 Aerodynamic size distribution of silica, chitosan and $CuSO_4$ particles

b) Detection of deposited porous particles

Ultraviolet visible (UV/VIS) spectroscopy was employed to detect $CuSO_4$ particles. The UV/VIS spectroscopy works on the principle of measuring ultraviolet or visible light absorption. When a molecule is exposed to a light having the energy that matches the electron transition energy, the electron is excited to a higher orbital while absorbing energy. Various compounds absorb maximum energies at different wavelengths depending on a type of electron transition that occurs, e.g. $CuSO_4$ absorbs maximum light energy in the region around 810 nm. The determination of the solution molar concentration is given by the Lamber–Beer law. Using this law, the amount of absorbed light can be correlated to a solution concentration. In our case, molar absorption coefficient of $CuSO_4$ at 810 nm was 14.85 L/mol/cm as can be seen in Figure 8.

At first, correlation between absorbance and concentration had to be determined. Aqueous solutions with known concentration of $CuSO_4$ (0.005, 0.01, 0.05, and 0.1 mol/L) were prepared. The absorbance was measured using a Spectrophotometer U-3900H (Hitachi, Tokyo, Japan). The method proved to be adequate for determining concentration of $CuSO_4$ as a linear relationship between absorbance and molar concentration of $CuSO_4$ (R^2=0.99) was observed (Figure 5).

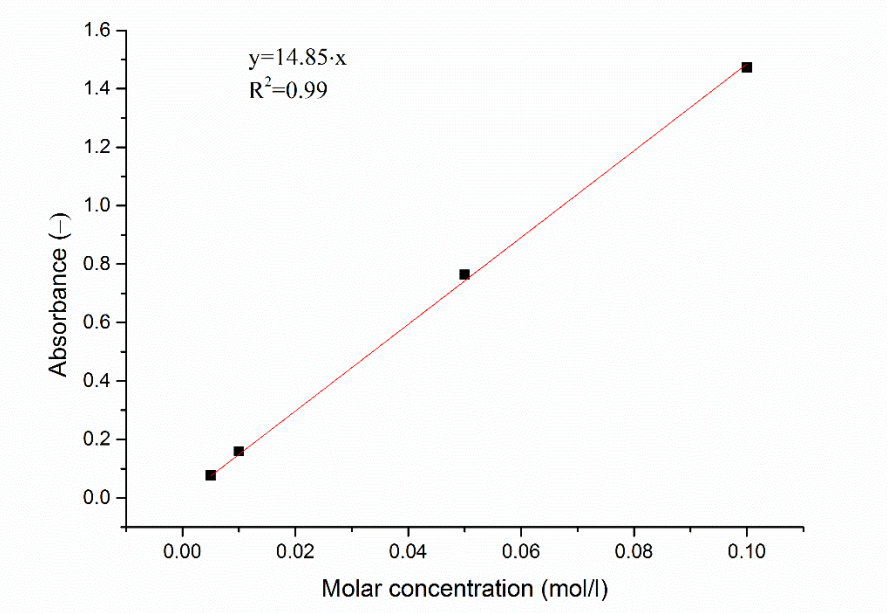

Figure 5 Absorbance of $CuSO_4$ as a function of molar concentration

c) Deposition measurements of porous particles

Deposition experiments were carried out using a realistic replica of human respiratory airways (Figure 6). The replica encompasses respiratory airways from the mouth to the 7th generation of bronchial branching (Lizal et al., 2012). The geometry was divided into 22 segments to permit regional deposition measurements. The numbering went from top to bottom starting with the oral cavity as number 1 and the trachea as number 2. The replica was manufactured using 3D printing.

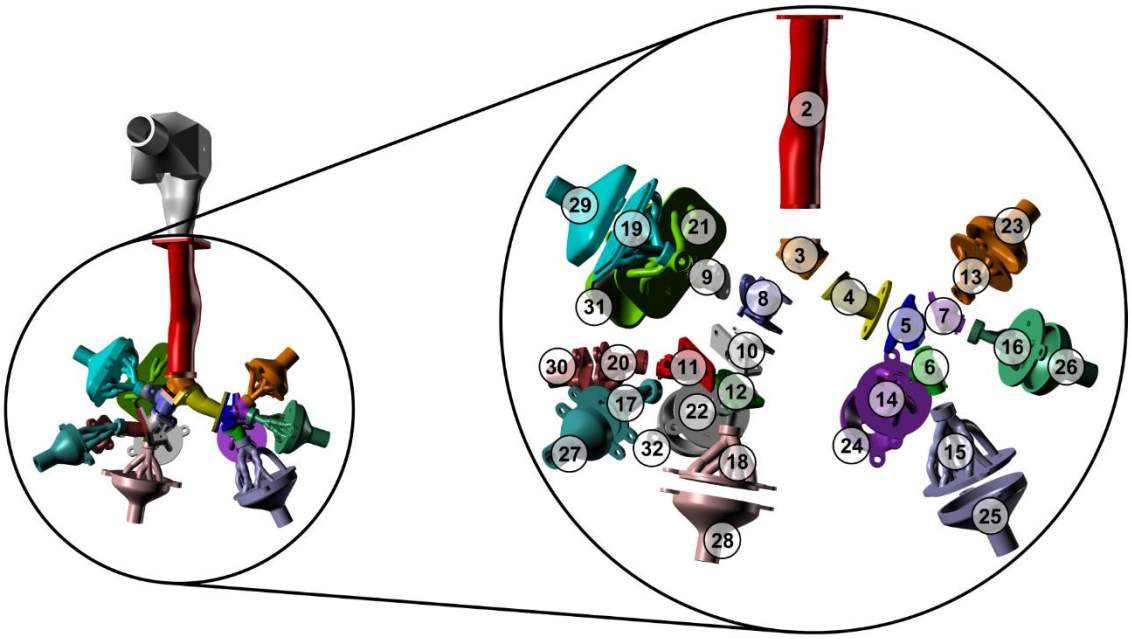

Figure 6 The replica of the respiratory airways (Lizal et al., 2015)

Leak test was performed prior to the deposition experiment because the replica consisted of multiple segments. Any leaks found, mostly between the flanges, were sealed with a small layer of silicone sealant.

After that, silicon oil (550 Fluid, Dow Corning) was poured into the replica and then dried out for 24 hours. Thus, a thin layer of silicon oil was created on the inner walls of the model to prevent resuspension of the deposited particles.

The experimental setup can be seen in Figure 7. The Small–Scale Powder Disperser 3433 (TSI, Shoreview, USA) was utilized to disperse the porous particles. The particles then flew through a dilutor where the air from the SSPD was mixed with additional filtered air to reach a desirable flow rate through the replica (the inspiratory flow rate was 30 L/min). After the dilutor, particles passed through the replica. Some of the particles deposited in the replica and the rest of them was collected on the output filters downstream of the model. The air through the replica was driven by the vacuum pump and the flow distribution through the individual branches was set via rotameters. The model exposition took 30 hours to deposit enough particles inside the replica.

The drawback of the method was that the output particle concentration from the SSPD was very low and a lot of particles deposited inside the SSPD or in the dilutor. The considerably high deposition in the dilutor also indicated that the particle size distribution measured during the particle production was different from the particle size distribution entering the replica. That is why the particle size distribution at the dilutor output was measured using the Aerodynamic Particle Sizer 3321 (TSI, Shoreview, USA). The measured CMAD was 1.41±2.1 μm and the MMAD was 8.15±1.6 μm. These values were used in the particle deposition calculations.

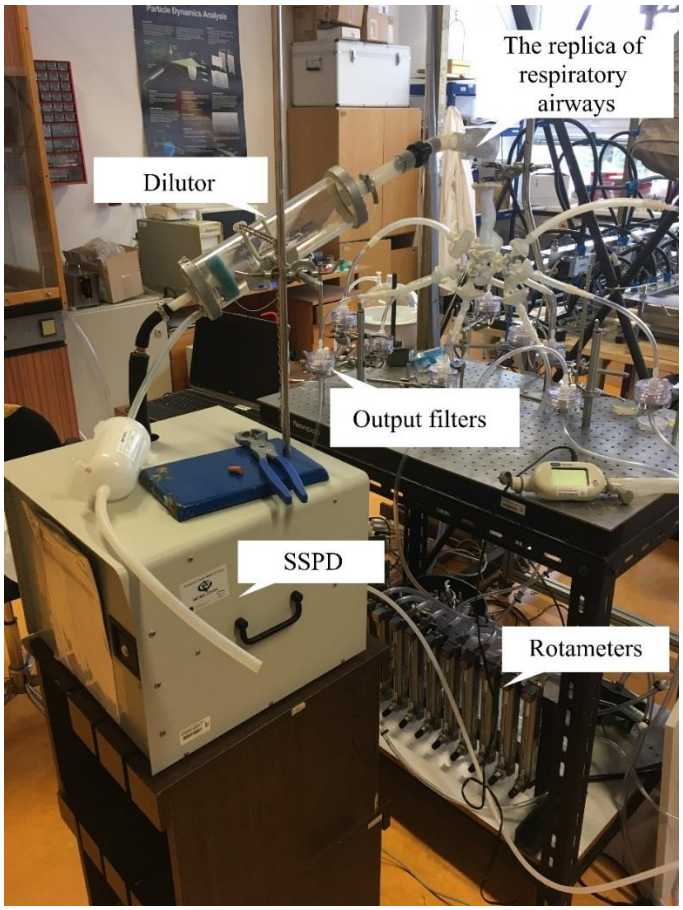

Figure 7 The experimental setup for deposition experiments

After the deposition experiment, the replica was disassembled and each segment was rinsed with a known volume of distilled water. The required volume to rinse a segment depended on the size and shape of the

segment. The resulting solutions were poured into plastic containers and these were placed into a sample box. The samples were analyzed using a Spectrophotometer U-3900H (Hitachi, Tokyo, Japan) and values of absorbance for each solution was obtained. These were used to calculate molar concentration of $CuSO_4$ in each sample. The actual mass of $CuSO_4$ deposited in each segment was calculated as

$$m = c_m \cdot V \cdot M \quad (1),$$

Where c_m is the molar concentration, V is volume of distilled water used for segment rinsing, and M is molar mass of $CuSO_4$ (M = 249.686 g/mol).

d) Results of porous particle deposition

Deposited mass in each segment was used for calculation of deposition characteristics, such as deposition fraction or deposition efficiency. Deposition fraction (DF) and deposition efficiency (DE) are given by equations 2 and 3:

$$\mathrm{DF} = \frac{deposited\ mass\ in\ a\ specific\ region}{total\ particle\ mass\ entering\ the\ oral\ airways} \quad (2),$$

$$\mathrm{DE} = \frac{deposited\ mass\ in\ a\ specific\ region}{total\ particle\ mass\ entering\ this\ region} \quad (3).$$

The fractional deposition was calculated for every segment of the replica and the results can be seen in Figure 8. The deposition fractions at the outputs of the replica represent deposited mass downstream of the replica, i.e. in the output funnel-shaped segments, in the tubing, and on the filters. However, the deposition fractions in these output parts were very low, under 1% in all cases. Most of the particles deposited within the lung replica, in particular in the oral cavity (62.6%) and the trachea (9.8%). Significant deposition was also around the first bifurcation and in the segments with the highest output flow rates (segments 15 and 18). The results indicated that the large porous particles were not able to follow the streamlines and deposited either in the oral cavity or around bifurcation of large respiratory airways.

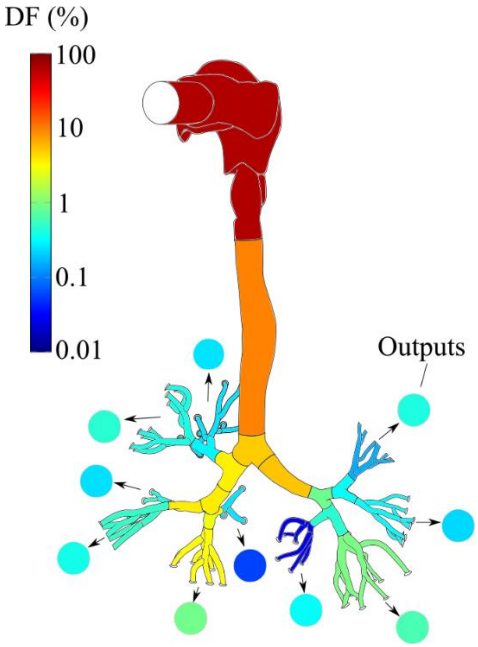

Figure 8 Deposition fractions in the replica; the output circles represent deposited mass in the output funnel-shaped segments, in the tubing and on the filters.

Deposition fraction as a function of segment number can be seen in Figure 9. The results of the current study were compared to the results of CFD simulation that was done on the same geometry (Koullapis et al., 2017). Koullapis et al. (2017) performed a large eddy simulation (LES) using a dynamic Smagorinsky turbulence model and implicit Euler particle tracking. The particle size was 10 µm with density of 0.914 g/cm^3. Using the equation 4, the aerodynamic diameter of these particles was 8.4 µm. The inspiratory flow rate was the same as in the experiment (30 L/min). The deposition patterns observed in the experimental results agreed to those predicted by the numerical simulations quite well. However, the deposition fraction differed slightly. The deposition in the oral cavity and in the trachea was higher during the experiment compared to the results of simulation. As most of the particles deposited in the upper respiratory airways, less particles reached the lower respiratory airways which caused lower deposition fraction in this part of the replica during experiment. This could be caused by the inlet velocity pattern. Turbulent inflow conditions were set in the simulation. However, it is impossible to say if these inlet conditions matched the conditions during the experiment without proper velocity measurements. Other reason for the deposition over prediction in the upper respiratory airways could be the particle size distribution. The porous particles were polydisperse which could result in significant deposition of large particles (larger than MMAD) in the oral cavity and the trachea and thus, very high deposition fraction. The advantage of numerical simulations is that all the particles have uniform size which is difficult to accomplish during experiments.

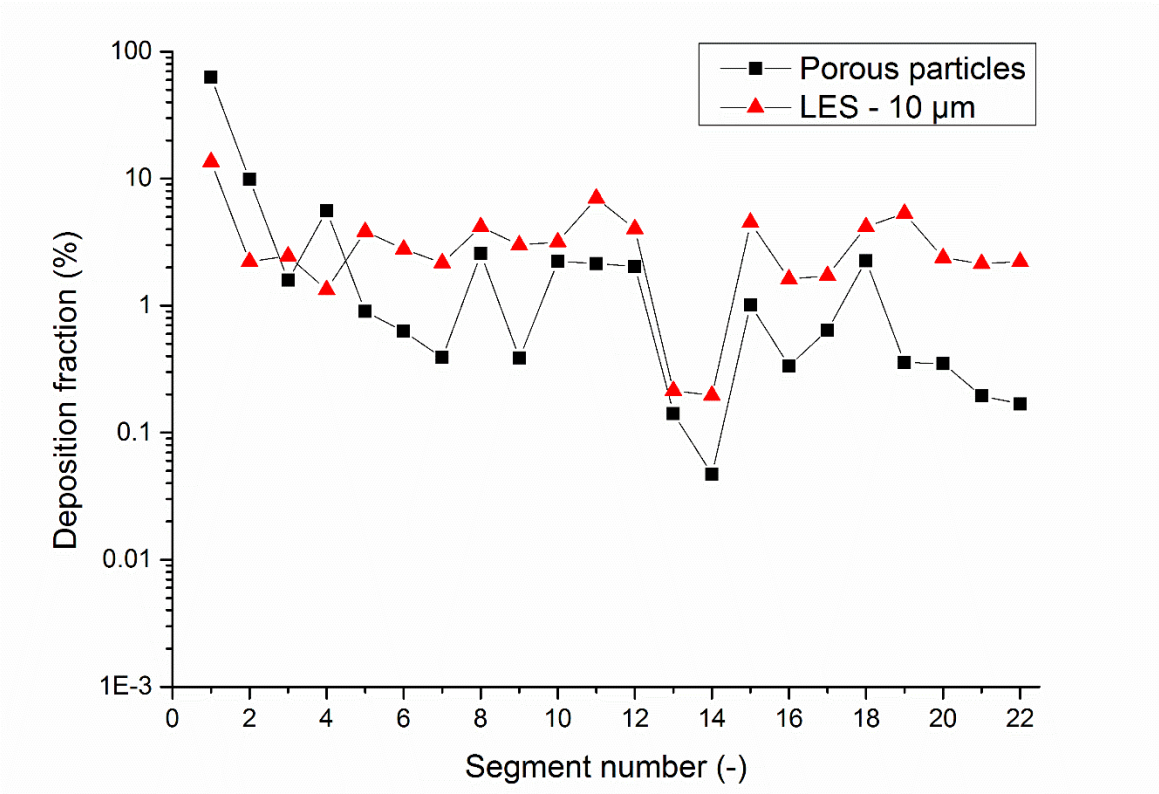

Figure 9 Comparison of deposition fraction as a function of segment number between experiment and numerical simulation

The particles did not deposit evenly in the respiratory airways but created so–called deposition hot spots. The deposition hot spots in the upper respiratory airways are depicted in Figure 10. For the clarity, the mean velocity field in the exact lung replica numerically investigated by Koullapis et al. (2017) is depicted as

well. The numerical simulation was done for the inhalation flow rate of 60 L/min. However, it is assumed that the flow field for the case of 30 L/min would differ only in velocity magnitudes. As the impaction was the main deposition mechanism, the deposition was highly affected by the flow field. The deposition hot spots were observed in the regions where the air turned rapidly, such as on the tongue, on the posterior wall of the oral cavity and larynx, and in the trachea. The deposition hot spots around the 1st bifurcation are depicted in Figure 11. A significant deposition was spotted on the carina of the bifurcation. The effect of the cartilage rings was observed in the main bronchi. The particles deposited in the protruding surfaces of the rings and created a "striped" deposition pattern. This effect was more significant after the bifurcation which was also observed in the study of Russo et al. (2008). In the smaller airways, deposition hot spots were mostly observed around carinas of the bifurcation. This trend went down to the 6th and 7th generation in which deposition around bifurcations was still noticeable.

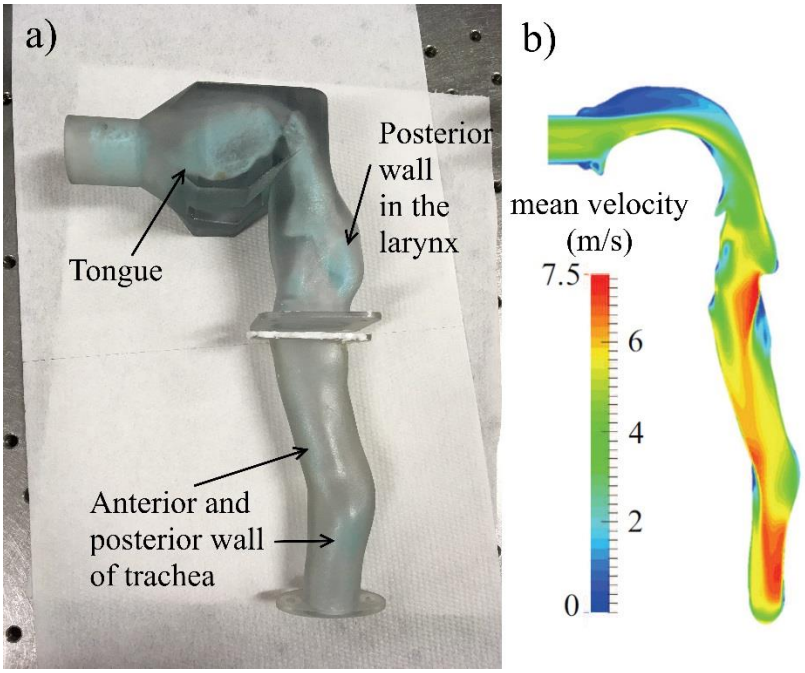

Figure 10 Deposition hot spots in the upper respiratory airways (a) and their agreement to flow field (b) at the inspiratory flow rate of 60 L/min (Koullapis et al., 2017)

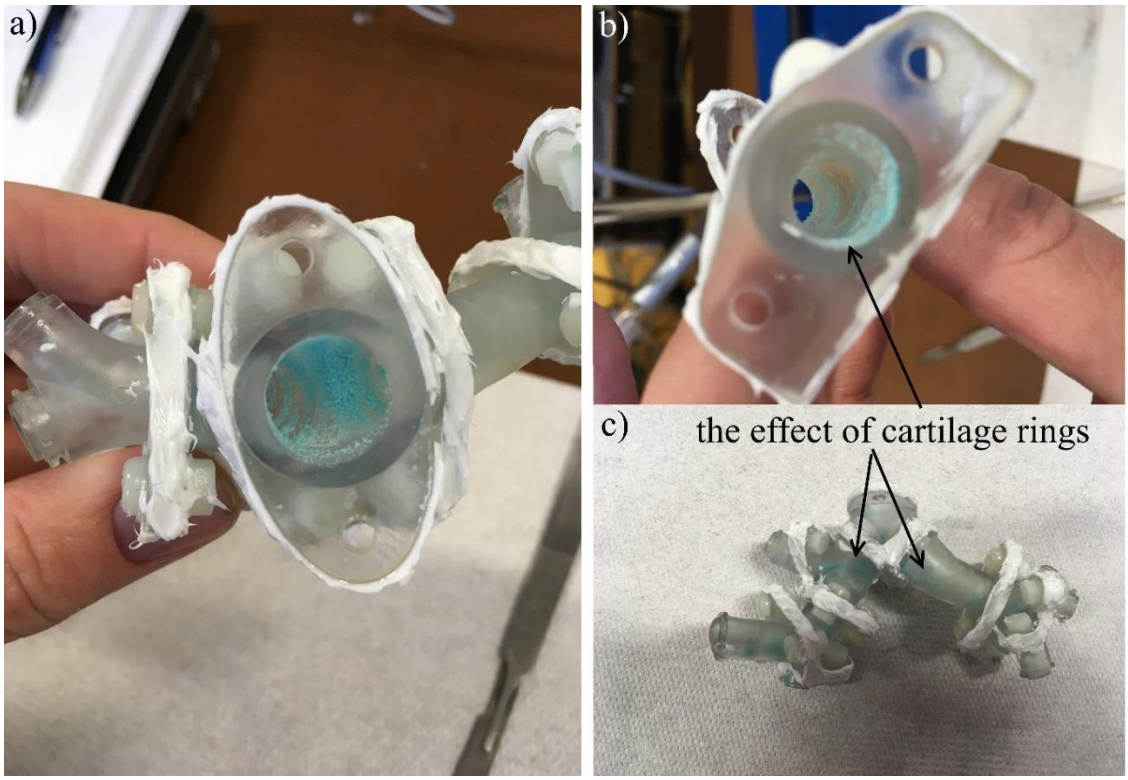

Figure 11 Deposition around the 1st bifurcation (a) and the effect of cartilage rings in the main bronchi (b, c)

Deposition efficiency as opposed to deposition fraction describes the ability of a given region to collect or filter particles. As the impaction mechanism has an important role in the upper respiratory tract and large conductive airways, deposition efficiency is frequently given as a function of impaction parameter (d_a^2Q) or Stokes number. Stokes number can be calculated using equation 4:

$$\mathrm{Stk} = \frac{\rho_0 \cdot d_a^2 \cdot v_i}{18 \cdot \eta \cdot D_i} \qquad (4)\ ,$$

where ρ_0 is water density, d_a is MMAD of the porous particles, and η denotes dynamic air viscosity. When calculating the Stokes number for particles flowing through the tracheobronchial tree, v_i represents the mean velocity in the trachea (segment 2) or the parent airway of the bifurcation (segment 3 to 12), and D_i is the mean diameter of the trachea or parent airway of the bifurcation. When calculating the Stokes number for aerosol flowing through the segment with multiple generations (segments 13–22), an output equivalent diameter was first calculated as an average of all output cross–sections from the given segment. Then, the average of input airway diameter and the output equivalent diameter were used as a mean diameter D_i. The mean velocity v_i in the given segment was calculated as the flow rate through the segment divided by its mean diameter D_i.

Deposition efficiency in the oral cavity as a function of impaction parameter is given in Figure 12. The deposition data of spherical particles from the study of Cheng et al. (1999) are presented for comparison. Our measurement showed higher deposition compared to the data from the other study. As in the previous chapters, this discrepancy could be caused either by the inlet conditions or polydispersity of porous particles. The polydispersity of particles is represented by a GSD. As GSD increases, the fraction of particles with diameter smaller than MMAD increases. On the other hand, the fraction of particles with diameter larger than MMAD also increases. Musante (2002) indicated, that for larger MMAD increasing GSD resulted in

enhanced deposition in the tracheobronchial tree and decreased deposition in the pulmonary region. As the deposition in the oral cavity is driven by the same mechanisms as the deposition in the tracheobronchial tree, it can be assumed that deposition increases with increasing GSD in this region.

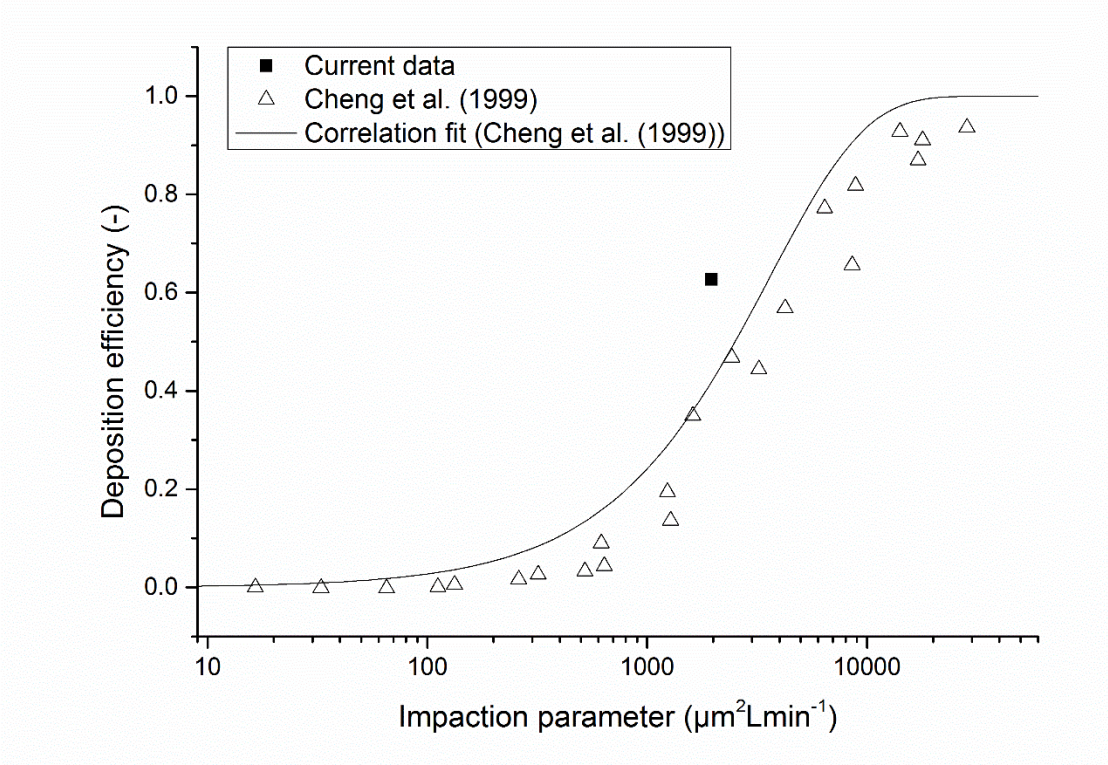

Figure 12 Deposition efficiency as a function of impaction parameter.

Deposition efficiency in the tracheobronchial tree as a function of Stokes number is depicted in Figure 13. The deposition efficiency increased with increasing Stokes number confirming the important role of impaction. The current data were compared to the data on spherical particle deposition measured by Chan and Lippmann (1980) and Zhou and Cheng (2005). Zhou and Cheng (2005) proposed empirical models for deposition of spherical particles in bifurcations from 1st to 4th generation of branching. These models are given by equation 5:

$$\mathrm{DE} = 1 - \exp(-5.39 \cdot F \cdot \mathrm{Stk}^{1.34}) \qquad (5)\,,$$

where F is the function of the bifurcation angle and the ratio of parent and daughter tube diameters. The values of F for various bifurcation were between values of 0.485 and 1.326 (solid lines in Figure 13). Our data agreed to the data from other studies quite well. Some of the data in the multigeneration segments overpredicted the deposition. This could be caused by the fact that "average" Stokes number had to be calculated for the segments encompassing several generation. Other reason can be the UV/VIS spectrometry method. As very low amounts of particles deposited in the small airways and on the output filters, the resulting concentrations were close to the detection limit of the method.

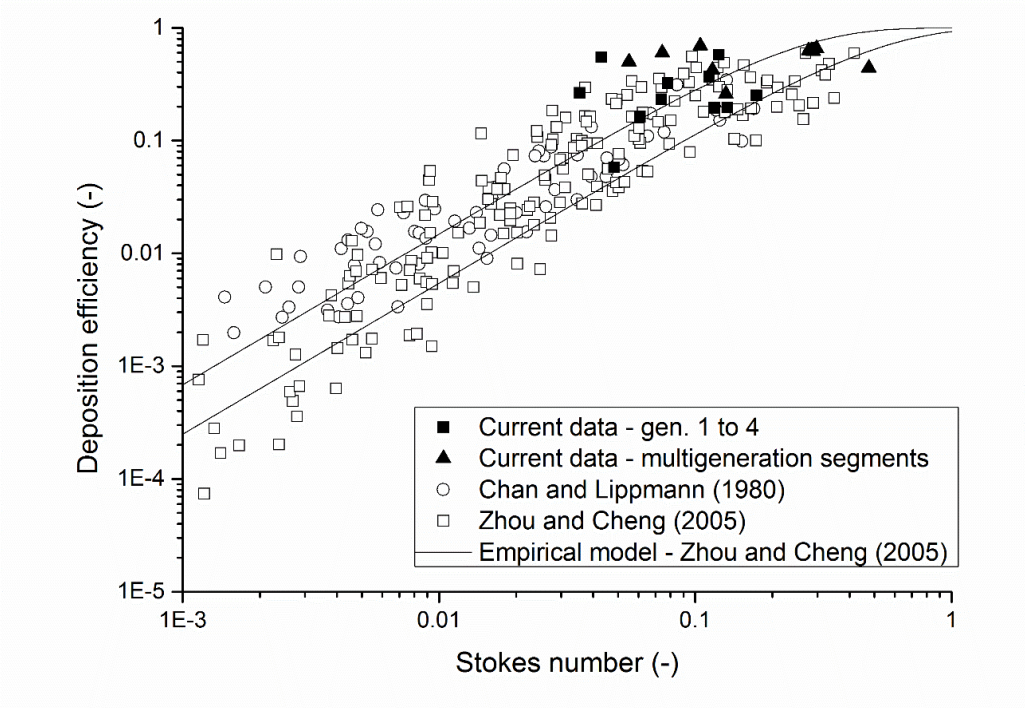

Figure 13 Deposition efficiency in the tracheobronchial tree as a function of Stokes number

The deposition of porous particles in the human airway replica was measured. The porous particles had rather high MMAD and thus, deposited significantly in the upper respiratory tract via impaction. When compared to other studies investigating deposition of spherical particles, the deposition characteristics agreed very well except the oral cavity. This indicated that porous particles deposited according to the aerodynamic diameter concept and the deposition is comparable to that of spherical particles. However, the effect of polydispersity on deposition should be studied in more detail.

3.1. Objective 2 - Deposition of fibrous particles

This chapter deals with fibrous particle deposition. The objective was to determine a deposition of fibrous particles. To do this, fibers with known size distribution had to be generated. The produced fibers were supposed to be introduced into the replica and deposit there. Proper detection method had to be found to quantify the regional particle deposition. Following paragraphs and figures were extracted from Belka et al. (2018).

a) Deposition experiments

The experimental setup for fiber deposition experiments is depicted in Figure 14. Uniform diameter fibers were classified according to their length using dielectrophoretic classifier (Wang et al., 2005). These classified fibers were introduced into the airway replica (Figure 6) at three steady inspiratory flow rates (15, 30 and 50 L/min). The airway replica was exposed to fibers for 4 hours. Since the replica did not include the entire lungs, some fibers passed through the replica and were collected on output filters. The output filters were changed every 30 min to prevent overfilling.

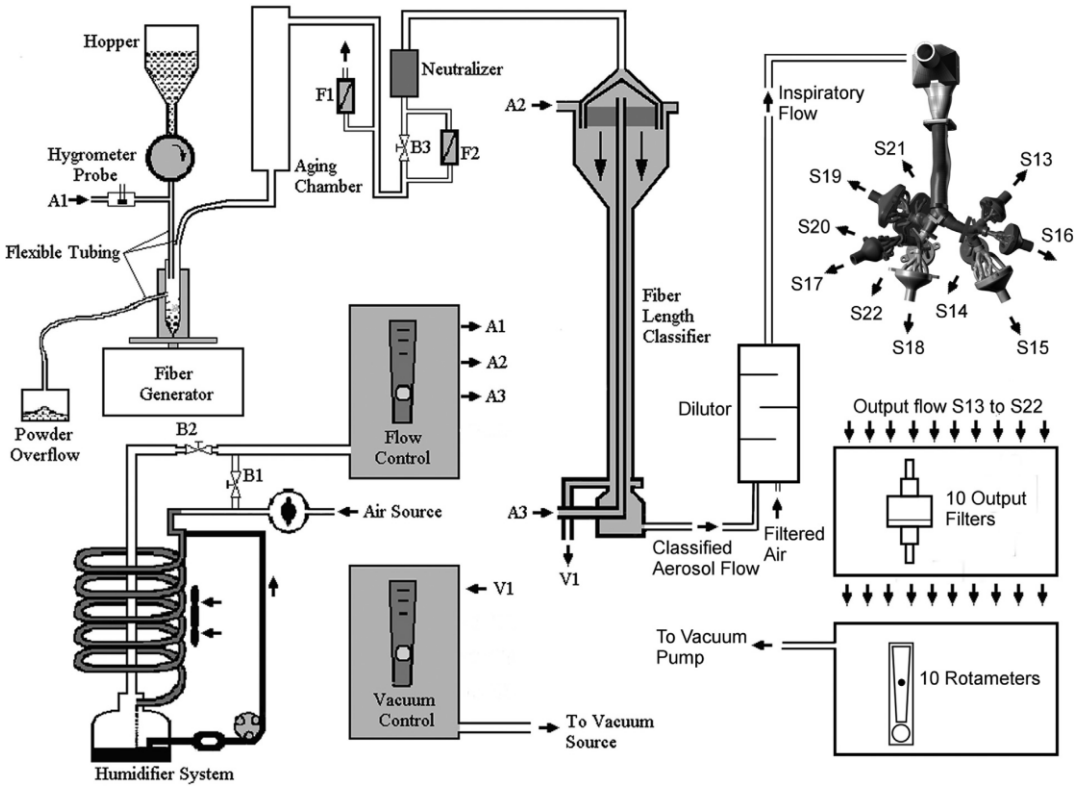

Figure 14 The experimental setup used for fiber deposition experiments

b) Sample preparation

Phase contrast microscopy was used for the sample analysis (Su and Cheng, 2005). The fibers deposited in the replica needed to be transferred to filters to permit counting. The replica was disassembled and each segment was put into a beaker with isopropanol (2-propanol, Fisher Scientific). The beaker with a segment was inserted into an ultrasonic bath and sonicated for one minute to release the fibers from the replica into the isopropanol. The resulting suspension was filtered through a membrane filter using a vacuum filtration unit. The filters were placed in a desiccator to dry.

An automatic image analysis method was employed to speed up the analysis, make it more convenient and more reproducible. A monochrome camera Atik 314E (Atik cameras, Norwich, UK) was attached to a microscope Nikon Eclipse E200 (Nikon, Tokyo, Japan) to take images of the filters. Twenty images of each filter were taken. As only a part of each filter was inspected this way, the counted numbers of fibers were then increased proportionally to account for the entire filter area. The images were analyzed with an in-house software Fiber Analyzer, which is able to identify and count fibers in filter images. The image analysis is based on the use of a histogram equalization and adaptive radial convolution filtering. The image analysis procedure is described in Belka et al. (2016). The steps of the analysis can be seen in Figure 15.

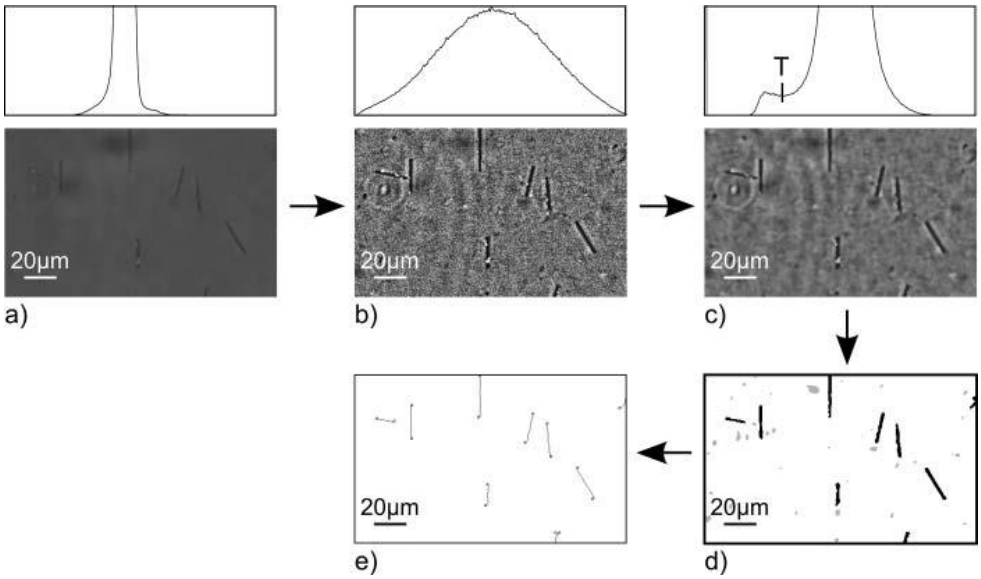

Figure 15 Image analysis procedure used to detect and count fibers

c) Deposition results

The fiber counts were employed in the calculation of deposition characteristics. Deposition efficiency and fraction were calculated using equations 2 and 3, respectively. The regional deposition fractions in the replica for the measured flow rates are shown in Figure 16. Deposition fractions at the replica outlets represent fractional depositions in the parts of the experimental setup downstream of the replica, i.e. funnel-like shaped segments, tubing and filters. Fibers deposited in these parts of the experimental setup penetrated the replica and would continue deeper into the lung. Only a few fibers actually deposited in the replica. The deposition fraction increased with an increasing flow rate, and the total deposition fractions in the replica were 0.7, 1.9 and 4.6% for the inspiratory flow rates of 15, 30, and 50 L/min, respectively. A slightly higher deposition fraction was detected in the oral cavity and in the complex segments. Moreover, segments in the right lung that encompassed a bifurcation in the fourth generation (segments 11 and 12) had a noticeably higher deposition fraction for higher inspiratory flow rates. By contrast, the complex segments downstream of the segments 11 and 12 had lower deposition fraction for higher inspiratory flow rate. This result indicated the role of impaction as the fibers were not able to follow streamlines into these complex segments and deposited near the carinal ridges.

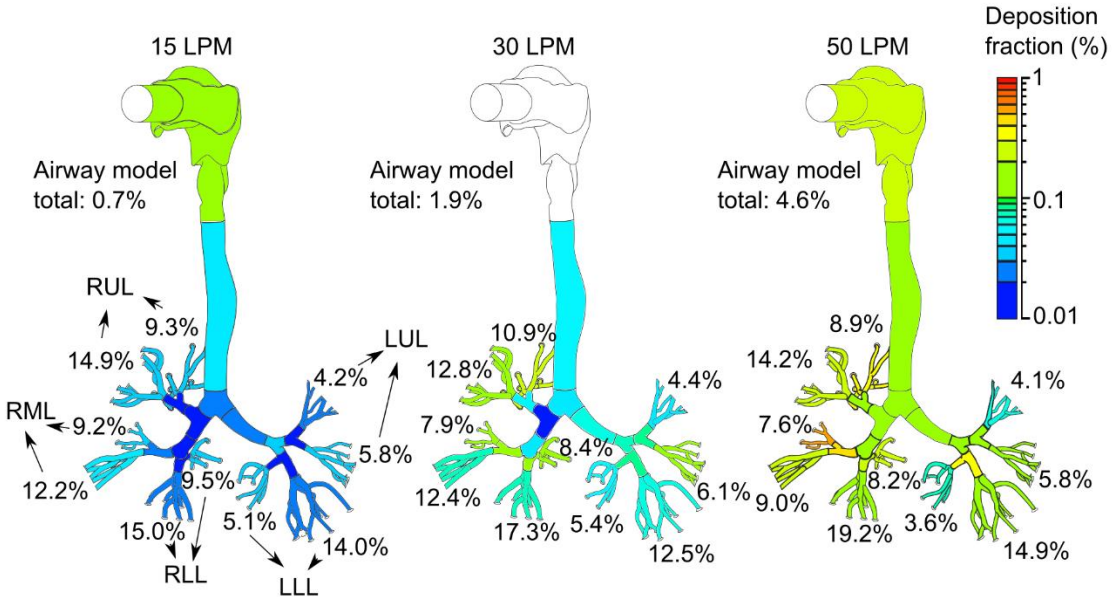

Figure 16 Regional deposition fractions in the replica as a function of flow rate; the values around the replica represent deposition fractions in the parts of the experimental setup downstream of the replica (the funnel-shaped output segments, the tubing, and the filters); the data for the oral cavity during 30 L/min study were excluded from the analysis

The deposition efficiencies were related to the Stokes number. The measured data were compared with those reported by Su and Cheng (2009) (casts A and B) and Su and Cheng (2015). Generally, the deposition efficiencies increased with the increasing Stokes number indicating the important role of impaction. The measured data were in good agreement with the literature results. The only exception of good agreement was the oral cavity. The examples of the result analysis can be seen in Figure 17 (deposition efficiency in the trachea and 1st generation as a function of Stokes number) and Figure 18 (deposition efficiency in the 3rd generation as the function of Stokes number).

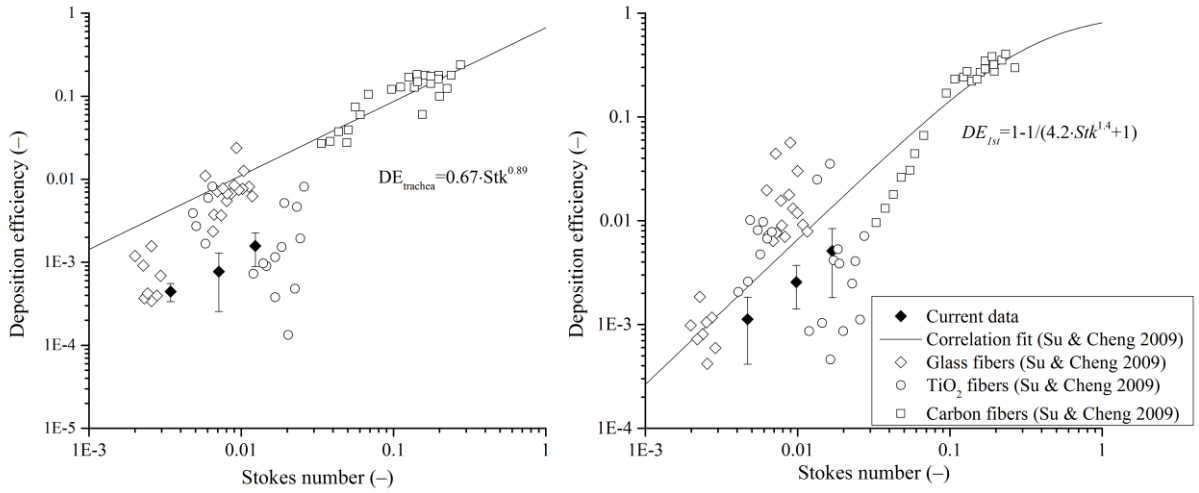

Figure 17 Deposition efficiency in the trachea (left) and 1st generation (right) as a function of Stokes number; the error bars represent standard deviations.

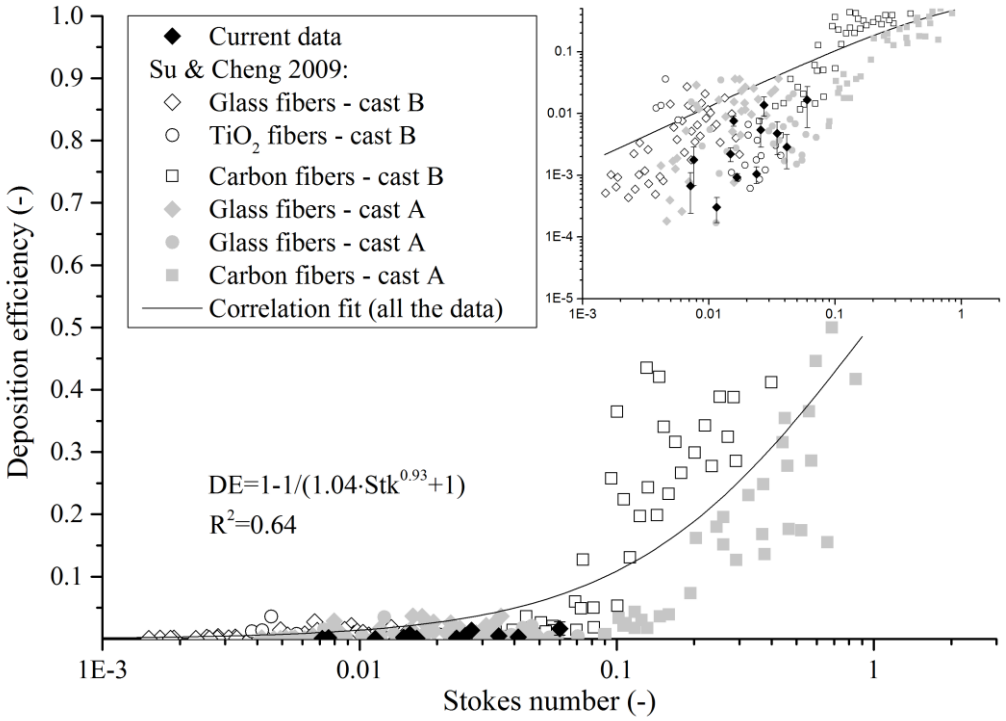

Figure 18 Deposition efficiency in the 3rd generation as a function of Stokes number; the error bars represent standard deviations.

Deposition in the 4th to 7th generation in the current respiratory airway replica can be seen in Figure 19. The 4th generation was incomplete and included only two bifurcations which were assumed to represent all the bifurcations in the 4th generation. The deposition efficiency increased with the increasing Stokes number even in the 4th generation. The measured data were also compared with the results of Myojo and Takaya (2001) and Zhou et al. (2007). Zhou et al. (2007) presented deposition of carbon fibers with a higher Stokes number than those in our study. However, our data followed the same trend. The deposition efficiencies reported by Myojo and Takaya (2001) were lower compared to the other studies. The deposition was measured in only one idealized bifurcation in their study. The smooth idealized walls together with the absence of upstream flow history likely caused the lower fiber deposition.

The other bifurcations in the 4th generation were part of the complex segments that extended down to the 6th or 7th generation. It was not possible to extract deposition per generation in these segments. Therefore, deposition efficiency for several generations as a function of average Stokes number is shown in Figure 19. Substantial variability was reported in the complex segments that included the same airway generations. This result indicated that the deposition was influenced by the upstream velocity fields and the individual segment geometry. The deposition efficiencies increased with increasing Stokes number, however, the increase was not that significant as in the case of more proximal generations. This result could be caused by the diminishing effect of impaction with increasing generation number. However, the use of average Stokes number is not ideal for this analysis and comparison with CFD results could provide additional insights.

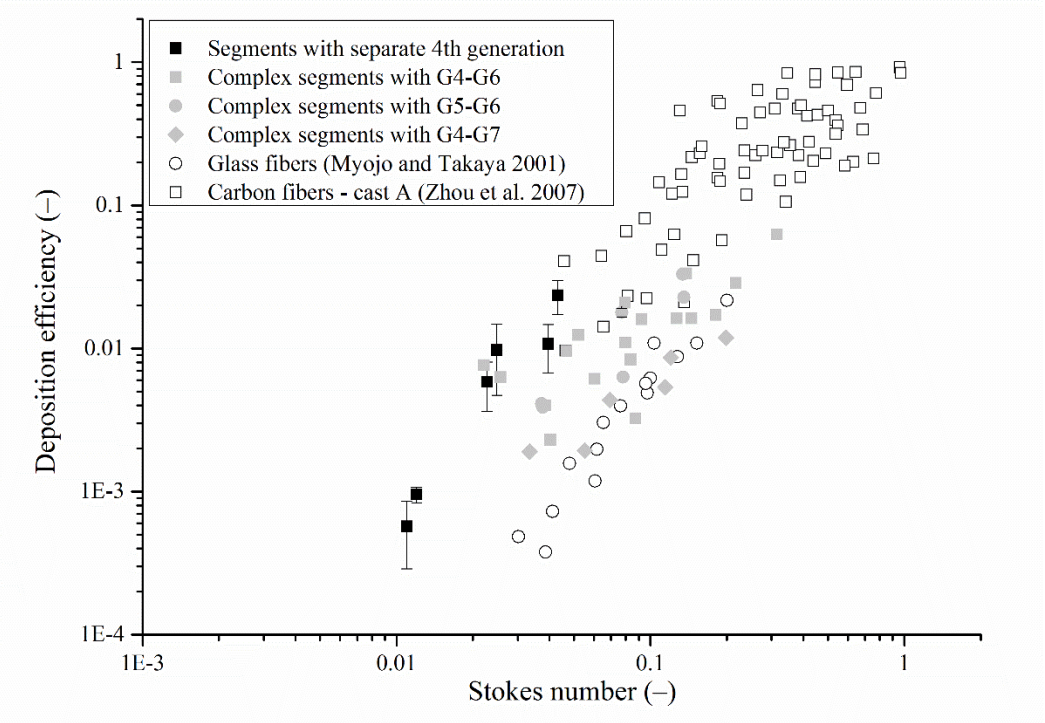

Figure 19 Deposition efficiency in the 4th to 7th generation as a function of Stokes number; the error bars represent standard deviations.

Deposition of fibers was compared to that of spherical particles. Lizal et al. (2015) carried out deposition experiments with radioactive spherical particles using the same airway replica. The Stokes numbers for the spherical particles were calculated using equation 4. The linear empirical model of Chan and Lippmann (1980) was also applied to the spherical particles data, and the fits for the data from first four generations were calculated. The same empirical model was used to calculate the fits for the fibrous particles. The deposition in the replicas was represented by equations 6 (R2=0.97) and 7 (R2=0.98), respectively.

$$DE_{spheres} = Stk^{1.038} \cdot 10^{0.0012} \quad (6)\ ,$$

$$DE_{fibers} = Stk^{1.452} \cdot 10^{0.0021} \quad (7)\ .$$

A comparison of particle deposition in the tracheobronchial tree together with the correlations are presented in Figure 20. Deposition of both particle types was driven by impaction since the deposition efficiency increased with the increasing Stokes number. Generally, deposition efficiency is higher for spherical particles than for the fibers having the same Stokes number. This result can be caused by the ability of fibers to align themselves with the airflow.

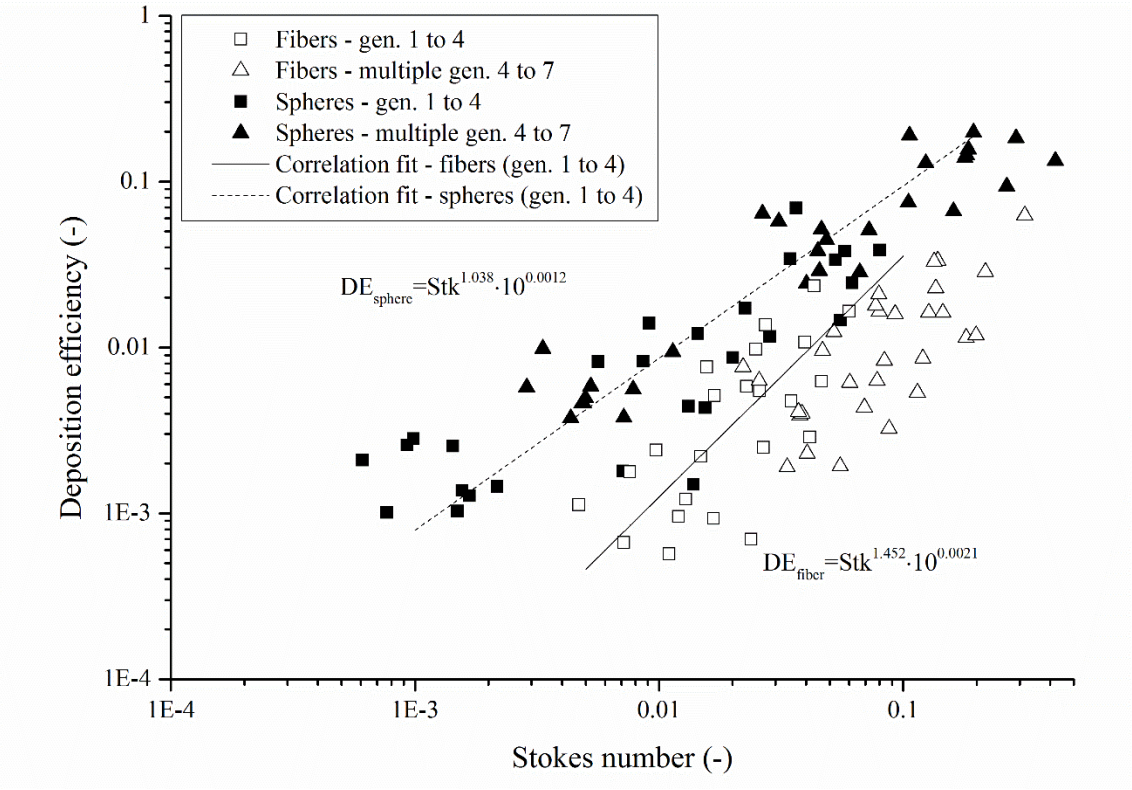

Figure 20 Deposition efficiency of fibrous and spherical particles as a function of Stokes number.

3.2. Summary

The deposition results of both porous and fibrous particles were analyzed. The results indicated that porous particles deposited as effectively as spherical particles. On the other hand, fibers deposited less effectively. Both formulated hypotheses were confirmed.

The deposition efficiencies of porous and fibrous particles as a function of Stokes number are depicted in Figure 21. The deposition results of spherical particles measured on the same airway replica are presented as well (Lizal et al., 2015). The empirical model used by Zhou et al. (2005) was employed to obtain empirical equations for various particles. OriginPro 9 (OriginLab Corporation, MA, USA) was utilized for this purpose. Only the deposition data measured in the segments encompassing single generation (gen. 1 to 4 of the replica) were employed for the curve fitting. The best curve fits for spherical and porous particles, and fibers are represented by equations 7 (R^2 = 0.45) and 8 (R^2 = 0.486), respectively:

$$\mathrm{DE}_{sphere,porous\ p.} = 1 - \exp(-5.14 \cdot \mathrm{Stk}^{1.3}) \quad (7),$$

$$\mathrm{DE}_{fibers} = 1 - \exp(-0.66 \cdot \mathrm{Stk}^{1.31}) \quad (8).$$

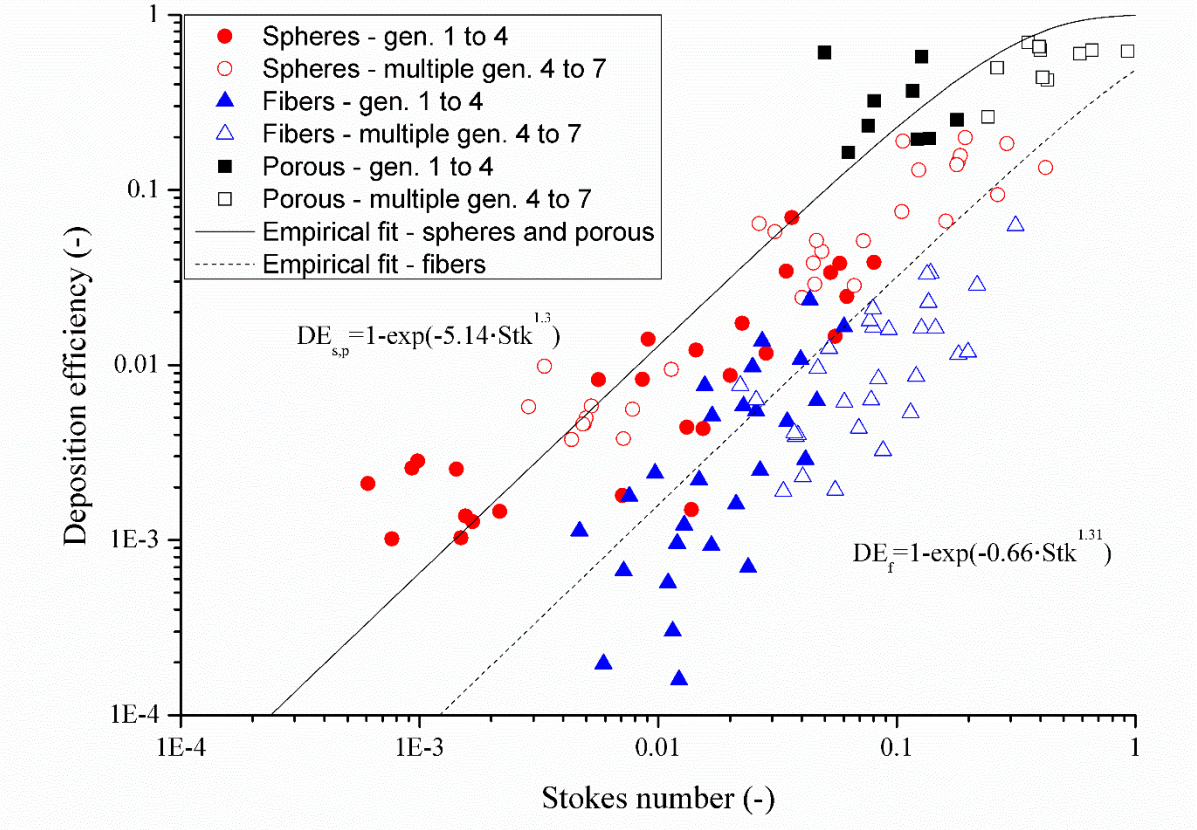

Figure 21 Deposition efficiencies of various particles as a function of Stokes number

Conclusions

Particle transport and deposition is highly studied topic nowadays. As the main attention of researchers has been deposition of spherical particles during normal breathing, this PhD thesis deals with regional deposition of non–spherical particles. The main goal was to analyze deposition of porous and fibrous particles.

The first objective was to study deposition of porous particles that have a big potential in inhalation therapy. Several methods for porous particle production were tested. The most suitable particles in the terms of size were obtained using spray–drying and liquid–liquid interface crystallization method. Chitosan particles with rather monodisperse size were produced by the spray–drying method. However, the total particle volume output was low and therefore, density measurements were not carried out. The crystallization method produced polydisperse particles made of $CuSO_4$ with sufficiently low density and porous structure. The mass median aerodynamic diameter of these particles was 8.15±1.6 μm and the bulk density was 0.42 g/cm^3. The $CuSO_4$ particles were utilized in deposition experiment at steady inhalation flow rate of 30 L/min. The deposition detection was performed using spectrophotometry.

As the MMAD of the particles was in micrometer scale, the deposition was driven mainly by impaction. This resulted in significant deposition fraction in the oral cavity (62,6%), the trachea (10%) and the main bronchi (7,2%). Comparing the deposition data to other studies using spherical particles, the deposition agreed very well except the oral cavity. The deposition of porous particles in the oral cavity was higher than that of spherical particles. This could be caused by the polydispersity of the particles.

The other objective was to study deposition of fibrous particles that are potentially hazardous for human health after inhalation. The glass fibers with density of 2.56 g/cm^3 and uniform diameter of 1.03±0.45 μm were classified according to their length using a dielectrophoretic classifier. After that, the fibers were introduced into the replica of respiratory airways at three steady inhalation flow rates (15, 30, and 50 L/min). The deposition detection was performed using phase–contrast microscopy. As the use of this method is very time–consuming and demanding for operator´s concentration, an automatic counting software based on the image processing was developed.

The deposition fraction of fibers was very low in the respiratory airway replica. The total deposition fractions were 0.7, 1.9, and 4.6% for inhalation flow rates of 15, 30, and 50 L/min, respectively. The deposition data agreed considerably well to available studies except the oral cavity. This time, the problem occurred during the sample preparation. The replica segments were sonicated to release the deposited fibers that were subsequently transferred onto filters. During the sonication, parts of the replica walls were released into the solution and these replica debris caused discrepancies during image analysis. This problem was observed only in the case of oral cavity as it was the largest segment with most released debris. Comparing the fiber deposition to that of spherical particles, fibers deposited less efficiently than spherical particles having the same Stokes number.

The current thesis contains original experimental results of non–spherical particles in the realistic replica of human respiratory airways from the oral cavity to 7th generation of branching. The amount of such a data in the literature is rather scarce and for example, fiber deposition beyond 4th generation has not been experimentally measured before. The deposition data confirmed that porous particles deposit as efficiently as spherical particles. On the other hand, fibers deposited less efficiently indicating that their aerodynamic behavior is of great importance. The formulated hypotheses of this thesis were confirmed.

The future research in this area can be aimed at measuring deposition of fibers having large Stokes numbers, i.e. fibers made of materials with higher density than glass or very long glass fibers having length approximately 100 μm. Further research can be aimed at deposition of polydisperse particles and their impact on deposition characteristics. The polydispersity is essential for inhalation therapy as the pharmaceutical aerosols are polydisperse. Experimental measurement using realistic breathing pattern for inhalation maneuver can be valuable.

References

Agu, R. U., Ugwoke, M. I., Armand, M., Kinget, R., & Verbeke, N. (2001). The lung as a route for systemic delivery of therapeutic proteins and peptides. *Respiratory Research, 2*(4), 198-209.

Altshuler, B. (1969). Behaviour of Airborne Particles in the Respiratory Tract *Ciba Foundation Symposium - Circulatory and Respiratory Mass Transport* (pp. 215-235): John Wiley & Sons, Ltd.

Asgharian, B., & Anjilvel, S. (1995a). The Effect of Fiber Inertia on Its Orientation in a Shear-Flow with Application to Lung Dosimetry. *Aerosol Science and Technology, 23*(3), 282-290. doi: Doi 10.1080/02786829508965313

Asgharian, B., & Anjilvel, S. (1995b). Movement and Deposition of Fibers in an Airway with Steady Viscous-Flow. *Aerosol Science and Technology, 22*(3), 261-270. doi: Doi 10.1080/02786829408959745

Asgharian, B., & Yu, C. P. (1989). A Simplified Model of Interceptional Deposition of Fibers at Airway Bifurcations. *Aerosol Science and Technology, 11*(1), 80-88. doi: Doi 10.1080/02786828908959301

Baron. (2001). Measurement of airborne particles-review. *Industrial Health*. Retrieved from http://202.241.32.9/en/indu_hel/pdf/IH39_08.pdf website:

Belka, M., Lizal, F., Jedelsky, J., Elcner, J., Hopke, P. K., & Jicha, M. (2018). Deposition of glass fibers in a physically realistic replica of the human respiratory tract. *Journal of Aerosol Science, 117*, 149-163. doi: 10.1016/j.jaerosci.2017.11.006

Belka, M., Lizal, F., Jedelsky, J., Starha, P., Druckmullerova, H., Hopke, P. K., & Jicha, M. (2016). Application of image analysis method to detection and counting of glass fibers from filter samples. *Aerosol Science and Technology, 50*(4), 353-362. doi: 10.1080/02786826.2016.1151858

Burney, P. G. J., Patel, J., Newson, R., Minelli, C., & Naghavi, M. (2015). Global and regional trends in COPD mortality, 1990-2010. *European Respiratory Journal, 45*(5), 1239-1247. doi: 10.1183/09031936.00142414

Byron, P. R., Hindle, M., Lange, C. F., Longest, P. W., McRobbie, D., Oldham, M. J., . . . Finlay, W. H. (2010). In vivo-in vitro correlations: predicting pulmonary drug deposition from pharmaceutical aerosols. *J Aerosol Med Pulm Drug Deliv, 23 Suppl 2*, S59-69. doi: 10.1089/jamp.2010.0846

Council of Europe (2007). *European Pharmacopoeia: Published in Accordance with the Convention on the Elaboration of a European Pharmacopoeia (European Treaty Series No. 50)*: Council of Europe.

Darquenne, C. (2012). Aerosol Deposition in Health and Disease. *Journal of Aerosol Medicine and Pulmonary Drug Delivery, 25*(3), 140-147. doi: DOI 10.1089/jamp.2011.0916

Dellamary, L. A., Tarara, T. E., Smith, D. J., Woelk, C. H., Adractas, A., Costello, M. L., . . . Weers, J. G. (2000). Hollow porous particles in metered dose inhalers. *Pharmaceutical Research, 17*(2), 168-174. doi: Doi 10.1023/A:1007513213292

Dunbar, C., Scheuch, G., Sommerer, K., DeLong, M., Verma, A., & Batycky, R. (2002). In vitro and in vivo dose delivery characteristics of large porous particles for inhalation. *International Journal of Pharmaceutics, 245*(1-2), 179-189. doi: 10.1016/s0378-5173(02)00349-6

Edwards, D., Hanes, J., Caponetti, G., Hrkach, J., BenJebria, A., Eskew, M., . . . Langer, R. (1997). Large porous particles for pulmonary drug delivery. [Article]. *Science, 276*(5320), 1868-1871. doi: 10.1126/science.276.5320.1868

Fan, F. G., & Ahmadi, G. (1995). A Sublayer Model for Wall Deposition of Ellipsoidal Particles in Turbulent Streams. *Journal of Aerosol Science, 26*(5), 813-840. doi: Doi 10.1016/0021-8502(95)00021-4

Feng, Y., & Kleinstreuer, C. (2013). Analysis of non-spherical particle transport in complex internal shear flows. *Physics of Fluids, 25*(9). doi: Artn 091904
10.1063/1.4821812

FIRS Forum of International Respiratory Societies, (2013). *Respiratory diseases in the world : realities of today - opportunities for tomorrow*.

Foord, N., Black, A., & Walsh, M. (1978). Regional deposition of 2.5–7.5 μm diameter inhaled particles in healthy male non-smokers. *Journal of Aerosol Science, 9*(4), 343-357. doi: http://dx.doi.org/10.1016/0021-8502(78)90037-X

Gervelas, C., Serandour, A. L., Geiger, S., Grillon, G., Fritsch, P., Taulelle, C., . . . Tsapis, N. (2007). Direct lung delivery of a dry powder formulation of DTPA with improved aerosolization properties: Effect on lung and systemic decorporation of plutonium. *Journal of Controlled Release, 118*(1), 78-86. doi: 10.1016/j.jconrel.2006.11.027

Gharse, S., & Fiegel, J. (2016). Large Porous Hollow Particles: Lightweight Champions of Pulmonary Drug Delivery. *Current Pharmaceutical Design, 22*(17), 2463-2469. doi: 10.2174/1381612822666160128145356

Gradon, L., & Sosnowski, T. R. (2014). Formation of particles for dry powder inhalers. *Advanced Powder Technology, 25*(1), 43-55. doi: DOI 10.1016/j.apt.2013.09.012

Grgic, B., Finlay, W. H., & Heenan, A. F. (2004). Regional aerosol deposition and flow measurements in an idealized mouth and throat. *Journal of Aerosol Science, 35*(1), 21-32. doi: Doi 10.1016/S0021-8502(03)00387-2

Harris, R. L., & Fraser, D. A. (1976). Model for Deposition of Fibers in Human Respiratory System. *American Industrial Hygiene Association Journal, 37*(2), 73-89. doi: Doi 10.1080/0002889768507416

Heyder, J., Armbruster, L., Gebhart, J., Grein, E., & Stahlhofen, W. (1975). Total deposition of aerosol particles in the human respiratory tract for nose and mouth breathing. *Journal of Aerosol Science, 6*(5), 311-328. doi: http://dx.doi.org/10.1016/0021-8502(75)90020-8

Heyder, J., Blanchard, J. D., Feldman, H. A., & Brain, J. D. (1988). Convective mixing in human respiratory tract: estimates with aerosol boli. *J Appl Physiol (1985), 64*(3), 1273-1278.

Heyder, J., Gebhart, J., Rudolf, G., Schiller, C. F., & Stahlhofen, W. (1986). Deposition of particles in the human respiratory tract in the size range 0.005–15 μm. *Journal of Aerosol Science, 17*(5), 811-825.

Hirst, P. H., Pitcairn, G. R., Weers, J. G., Tarara, T. E., Clark, A. R., Dellamary, L. A., . . . Newman, S. P. (2002). In vivo lung deposition of hollow porous particles from a pressurized metered dose inhaler. *Pharmaceutical Research, 19*(3), 258-264. doi: Doi 10.1023/A:1014482615914

Hofmann, W. (2011). Modelling inhaled particle deposition in the human lung—A review. *Journal of Aerosol Science, 42*(10), 693-724. doi: 10.1016/j.jaerosci.2011.05.007

Chan, T. L., & Lippmann, M. (1980). EXPERIMENTAL MEASUREMENTS AND EMPIRICAL MODELING OF THE REGIONAL DEPOSITION OF INHALED PARTICLES IN HUMANS. *American Industrial Hygiene Association Journal, 41*(6), 399-408. doi: 10.1080/15298668091424942

Cheng, K. H., Cheng, Y. S., Yeh, H. C., & Swift, D. L. (1997). An experimental method for measuring aerosol deposition efficiency in the human oral airway. *American Industrial Hygiene Association Journal, 58*(3), 207-213. doi: Doi 10.1202/0002-8894(1997)058<0207:Aemfma>2.0.Co;2

Cheng, Y. S. (2014). Mechanisms of pharmaceutical aerosol deposition in the respiratory tract. *AAPS PharmSciTech, 15*(3), 630-640. doi: 10.1208/s12249-014-0092-0

Cheng, Y. S., Zhou, Y., & Chen, B. T. (1999). Particle deposition in a cast of human oral airways. *Aerosol Science and Technology, 31*(4), 286-300. doi: Doi 10.1080/027868299304165

Inthavong, K., Mouritz, A. P., Dong, J. L., & Tu, J. Y. (2013). Inhalation and deposition of carbon and glass composite fibre in the respiratory airway. *Journal of Aerosol Science, 65*, 58-68. doi: 10.1016/j.jaerosci.2013.07.003

Jeffery, G. B. (1922). The Motion of Ellipsoidal Particles Immersed in a Viscous Fluid. [10.1098/rspa.1922.0078]. *Proceedings of the Royal Society of London. Series A, 102*(715), 161.

Kim, C. S., Hu, S. C., DeWitt, P., & Gerrity, T. R. (1996). Assessment of regional deposition of inhaled particles in human lungs by serial bolus delivery method. *Journal of Applied Physiology, 81*(5), 2203-2213.

Kleinstreuer, C., & Feng, Y. (2013). Computational Analysis of Non-Spherical Particle Transport and Deposition in Shear Flow With Application to Lung Aerosol Dynamics-A Review. *Journal of Biomechanical Engineering-Transactions of the Asme, 135*(2). doi: Artn 021008
Doi 10.1115/1.4023236
Kleinstreuer, C., Zhang, Z., & Donohue, J. F. (2008). Targeted drug-aerosol delivery in the human respiratory system. *Annu Rev Biomed Eng, 10*, 195-220. doi: 10.1146/annurev.bioeng.10.061807.160544
Koullapis, P., Kassinos, S. C., Muela, J., Perez-Segarra, C., Rigola, J., Lehmkuhl, O., . . . Nicolaou, L. (2017). Regional aerosol deposition in the human airways: The SimInhale benchmark case and a critical assessment of in silico methods. *European Journal of Pharmaceutical Sciences*. doi: https://doi.org/10.1016/j.ejps.2017.09.003
Lambert, A. R., O'Shaughnessy, P., Tawhai, M. H., Hoffman, E. A., & Lin, C. L. (2011). Regional deposition of particles in an image-based airway model: large-eddy simulation and left-right lung ventilation asymmetry. *Aerosol Sci Technol, 45*(1), 11-25. doi: 10.1080/02786826.2010.517578
Laumbach, R. J., & Kipen, H. M. (2012). Respiratory health effects of air pollution: Update on biomass smoke and traffic pollution. *Journal of Allergy and Clinical Immunology, 129*(1), 3-13. doi: 10.1016/j.jaci.2011.11.021
Lizal, F., Belka, M., Adam, J., Jedelsky, J., & Jicha, M. (2015). A method for in vitro regional aerosol deposition measurement in a model of the human tracheobronchial tree by the positron emission tomography. *Proceedings of the Institution of Mechanical Engineers Part H-Journal of Engineering in Medicine, 229*(10), 750-757. doi: 10.1177/0954411915600005
Lizal, F., Elcner, J., Hopke, P. K., Jedelsky, J., & Jicha, M. (2012). Development of a realistic human airway model. *Proceedings of the Institution of Mechanical Engineers Part H-Journal of Engineering in Medicine, 226*(H3), 197-207. doi: 10.1177/0954411911430188
Longest, P. W., & Holbrook, L. T. (2012). In silico models of aerosol delivery to the respiratory tract - development and applications. *Adv Drug Deliv Rev, 64*(4), 296-311. doi: 10.1016/j.addr.2011.05.009
Longest, P. W., & Xi, J. X. (2007). Effectiveness of direct Lagrangian tracking models for simulating nanoparticle deposition in the upper airways. *Aerosol Science and Technology, 41*(4), 380-397. doi: 10.1080/02786820701203223
Mitchell, J., Newman, S., & Chan, H. K. (2007). In Vitro and In Vivo Aspects of Cascade Impactor Tests and Inhaler Performance: A Review. *Aaps Pharmscitech, 8*(4).
Mitchell, J. P., & Nagel, M. W. (2003). Cascade impactors for the size characterization of aerosols from medical inhalers: Their uses and limitations. *Journal of Aerosol Medicine-Deposition Clearance and Effects in the Lung, 16*(4), 341-+. doi: Doi 10.1089/089426803772455622
Muir, D. C., Sweetland, K., & Love, R. G. (1970). Inhaled aerosol boluses in man. *Inhaled Part, 1*, 81-90.
Musante, C. J., Schroeter, J. D., Rosati, J. A., Crowder, T. M., Hickey, A. J., & Martonen, T. B. (2002). Factors affecting the deposition of inhaled porous drug particles. *Journal of Pharmaceutical Sciences, 91*(7), 1590-1600. doi: 10.1002/jps.10152
Myojo, T. (1987). Deposition of Fibrous Aerosol in Model Bifurcating Tubes. *Journal of Aerosol Science, 18*(3), 337-&. doi: Doi 10.1016/0021-8502(87)90027-9
Myojo, T. (1990). The Effect of Length and Diameter on the Deposition of Fibrous Aerosol in a Model Lung Bifurcation. *Journal of Aerosol Science, 21*(5), 651-659. doi: Doi 10.1016/0021-8502(90)90120-M
Myojo, T., & Takaya, M. (2001). Estimation of fibrous aerosol deposition in upper bronchi based on experimental data with model bifurcation. *Industrial Health, 39*(2), 141-149. doi: DOI 10.2486/indhealth.39.141
Nolan, L. M., Tajber, L., McDonald, B. F., Barham, A. S., Corrigan, O. I., & Healy, A. M. (2009). Excipient-free nanoporous microparticles of budesonide for pulmonary delivery. *European Journal of Pharmaceutical Sciences, 37*(5), 593-602. doi: 10.1016/j.ejps.2009.05.007

Oberdorster, G., Sharp, Z., Atudorei, V., Elder, A., Gelein, R., Kreyling, W., & Cox, C. (2004). Translocation of inhaled ultrafine particles to the brain. *Inhalation Toxicology, 16*(6-7), 437-445. doi: 10.1080/08958370490439597

Pirozynski, M., & Sosnowski, T. R. (2016). Inhalation devices: from basic science to practical use, innovative vs generic products. *Expert Opinion on Drug Delivery, 13*(11), 1559-1571. doi: 10.1080/17425247.2016.1198774

Rostami, A. A. (2009). Computational Modeling of Aerosol Deposition in Respiratory Tract: A Review. *Inhalation Toxicology, 21*(4), 262-290. doi: 10.1080/08958370802448987

Russo, J., Robinson, R., & Oldham, M. J. (2008). Effects of cartilage rings on airflow and particle deposition in the trachea and main bronchi. *Med Eng Phys, 30*(5), 581-589. doi: 10.1016/j.medengphy.2007.06.010

Shanley, K. T., & Ahmadi, G. (2011). A Numerical Model for Simulating the Motions of Ellipsoidal Fibers Suspended in Low Reynolds Number Shear Flows. *Aerosol Science and Technology, 45*(7), 838-848. doi: 10.1080/02786826.2011.566293

Shanley, K. T., Ahmadi, G., Hopke, P. K., & Cheng, Y.-S. (2016). Simulated airflow and rigid fiber behavior in a realistic nasal airway model. *Particulate Science and Technology*, 1-10. doi: 10.1080/02726351.2016.1208694

Shoyele, S. A., & Cawthome, S. (2006). Particle engineering techniques for inhaled biopharmaceuticals. *Advanced Drug Delivery Reviews, 58*(9-10), 1009-1029. doi: DOI 10.1016/j.addr.2006.07.010

Schiller-Scotland, C. F., Hlawa, R., & Gebhart, J. (1994). Experimental-Data for Total Deposition in the Respiratory-Tract of Children. *Toxicology Letters, 72*(1-3), 137-144. doi: Doi 10.1016/0378-4274(94)90020-5

Stahlhofen, W., Rudolf, G., & James, A. C. (1989). Intercomparison of Experimental Regional Aerosol Deposition Data. *Journal of Aerosol Medicine, 2*(3), 285-308. doi: 10.1089/jam.1989.2.285

Su, W. C., & Cheng, Y. S. (2005). Deposition of fiber in the human nasal airway. *Aerosol Science and Technology, 39*(9), 888-901. doi: 10.1080/02786820500295685

Su, W. C., & Cheng, Y. S. (2006). Fiber deposition pattern in two human respiratory tract replicas. *Inhalation Toxicology, 18*(10), 749-760. doi: 10.1080/08958370600748513

Su, W. C., & Cheng, Y. S. (2009). Deposition of man-made fibers in human respiratory airway casts. *Journal of Aerosol Science, 40*(3), 270-284. doi: 10.1016/j.jaerosci.2008.11.003

Su, W. C., & Cheng, Y. S. (2015). Estimation of carbon nanotubes deposition in a human respiratory tract replica. *Journal of Aerosol Science, 79*, 72-85. doi: 10.1016/j.jaerosci.2014.09.005

Sussman, R. G., Cohen, B. S., & Lippmann, M. (1991). Asbestos Fiber Deposition in a Human Tracheobronchial Cast. I. Experimental. *Inhalation Toxicology, 3*(2), 145-160. doi: doi:10.3109/08958379109145281

Tian, L., & Ahmadi, G. (2013). Fiber transport and deposition in human upper tracheobronchial airways. *Journal of Aerosol Science, 60*, 1-20. doi: 10.1016/j.jaerosci.2013.02.001

Tian, L., Ahmadi, G., Wang, Z., & Hopke, P. K. (2012). Transport and deposition of ellipsoidal fibers in low Reynolds number flows. *Journal of Aerosol Science, 45*, 1-18. doi: 10.1016/j.jaerosci.2011.09.001

Tian, L., Shang, Y., Chen, R., Bai, R., Chen, C. Y., Inthavong, K., & Tu, J. Y. (2017). A combined experimental and numerical study on upper airway dosimetry of inhaled nanoparticles from an electrical discharge machine shop. *Particle and Fibre Toxicology, 14*. doi: ARTN 24
10.1186/s12989-017-0203-7

Vanbever, R., Mintzes, J., Wang, J., Nice, J., Chen, D., Batycky, R., . . . Edwards, D. (1999). Formulation and physical characterization of large porous particles for inhalation. [Article]. *Pharmaceutical Research, 16*(11), 1735-1742. doi: 10.1023/A:1018910200420

Versteeg, H. K., & Malalasekera, W. (2007). *An introduction to computational fluid dynamics : the finite volume method* (2nd ed. ed.). Harlow: Prentice Hall.

Wang, Z., Hopke, P. K., Baron, P. A., Ahmadi, G., Cheng, Y.-S., Deye, G., & Su, W.-C. (2005). Fiber Classification and the Influence of Average Air Humidity. *Aerosol Science and Technology, 39*(11), 1056-1063. doi: 10.1080/02786820500380198

Weibel, E. R. (1963). *Morphometry of the human lung*. Berlin: [s.n.].

Zhang, L., Asgharian, B., & Anjilvel, S. (1996). Inertial and interceptional deposition of fibers in a bifurcating airway. *Journal of Aerosol Medicine-Deposition Clearance and Effects in the Lung, 9*(3), 419-430. doi: DOI 10.1089/jam.1996.9.419

Zhang, Y., Finlay, W. H., & Matida, E. A. (2004). Particle deposition measurements and numerical simulation in a highly idealized mouth-throat. *Journal of Aerosol Science, 35*(7), 789-803. doi: 10.1016/j.jaerosci.2003.12.006

Zhou, Y., & Cheng, Y. (2005). Partical deposition in a cast of human tracheobronchial airways. *Aerosol science and technology, 39*, 492-500.

Zhou, Y., Su, W. C., & Cheng, Y. S. (2007). Fiber deposition in the tracheobronchial region: Experimental measurements. *Inhalation Toxicology, 19*(13), 1071-1078. doi: 10.1080/08958370701626634

List of publications

Papers published in journals with impact factor

- BĚLKA, M.; LÍZAL, F.; JEDELSKÝ, J.; ŠTARHA, P.; DRUCKMÜLLEROVÁ, H.; JÍCHA, M. Application of image analysis method to detection and counting of glass fibers from filter samples. AEROSOL SCIENCE AND TECHNOLOGY, 2016, vol. 50, no. 4, p. 352-363. ISSN: 0278-6826.
- BĚLKA, M.; LÍZAL, F.; JEDELSKÝ, J.; ELCNER, J.; HOPKE, P.; JÍCHA, M. Deposition of glass fibers in a physically realistic replica of the human respiratory tract. JOURNAL OF AEROSOL SCIENCE, 2017, no. 1, p. 1-15. ISSN: 0021-8502.
- LÍZAL, F.; BĚLKA, M.; ADAM, J.; JEDELSKÝ, J.; JÍCHA, M. A method for in vitro regional aerosol deposition measurement in a model of the human tracheobronchial tree by the positron emission tomography. PROCEEDINGS OF THE INSTITUTION OF MECHANICAL ENGINEERS PART H-JOURNAL OF ENGINEERING IN MEDICINE, 2015, vol. 229, no. 10, p. 750-757. ISSN: 0954-4119.
- NORDLUND, M.; BĚLKA, M.; KUCZAJ, A.; LÍZAL, F.; JEDELSKÝ, J.; ELCNER, J.; JÍCHA, M. Multicomponent aerosol particle deposition in a realistic cast of the human upper respiratory tract. Inhalation Toxicology, 2017, vol. 29, no. 3, p. 113-125. ISSN: 1091-7691.
- FREDERIX, E.; KUCZAJ, A.; NORDLUND, M.; BĚLKA, M.; LÍZAL, F.; JEDELSKÝ, J.; ELCNER, J.; JÍCHA, M.; GEURTS, B. Simulation of size-dependent aerosol deposition in a realistic model of the upper human airways. JOURNAL OF AEROSOL SCIENCE, 2017, vol. 115, no. 1, p. 29-45. ISSN: 0021-8502.

Papers from conference proceedings listed in CPCI Thomson Reuters database or Scopus

- BĚLKA, M.; LÍZAL, F.; JEDELSKÝ, J.; JÍCHA, M. Analysis of fiber deposition using automatic image processing method. In International Conference Experimental Fluid Mechanics 2012 Conference proceedings. EPJ Web of Conferences. FRANCE: E D P SCIENCES, 2013. p. 1-4. ISBN: 978-80-7372-912-7. ISSN: 2100-014X.
- BĚLKA, M.; LIPPAY, J.; LÍZAL, F.; JEDELSKÝ, J.; JÍCHA, M. Comparison of methods for evaluation of aerosol deposition in the model of human lungs. In EPJ Web of Conferences. EPJ Web of Conferences. FRANCE: E D P SCIENCES, 2014. p. 82-85. ISBN: 978-80-260-5375-0. ISSN: 2100-014X.
- BĚLKA, M.; JEDELSKÝ, J.; ZAREMBA, M.; MALÝ, M.; LÍZAL, F. Measurement of Air Flow in Trachea Using Particle Image Velocimetry and Laser-Doppler Anemometry. In Engineering Mechanics 2014. Engineering mechanics 2014. 1. Svratka: 2014. p. 72-75. ISBN: 978-80-214-4871-1. ISSN: 1805-8248.
- BĚLKA, M.; JEDELSKÝ, J.; ELCNER, J. Measurement of Cyclic Flows in Trachea Using PIV and Numerical simulation. In EPJ Web of Conferences. EPJ Web of Conferences. France: EDP Sciences, 2015. p. 1-4. ISSN: 2100-014X.
- BĚLKA, M.; LÍZAL, F.; JEDELSKÝ, J.; JÍCHA, M.; POSPÍŠIL, J. Measurement of an electronic cigarette aerosol size distribution during a puff. In EPJ Web of Conferences. EPJ Web of Conferences. France: EDP SCIENCES, 2017. p. 1-4. ISSN: 2100-014X.

CURRICULUM VITAE

Ing. Miloslav Bělka

Date and place of birth: 5th of July, 1998, Kroměříž

Education:

2012–2018 BUT, Faculty of Mechanical Engineering – Design and process engineering

Doctoral studies

- Experimental study of particle transport and deposition in the human respiratory tract (the effect of flow field and particle characteristics)

.

2010–2012 BUT, Faculty of Mechanical Engineering – Environmental engineering

Master degree studies

- Study of systems used to provide thermal comfort and indoor air quality (ventilation, air-conditioning, and heating) and principles they are based on (mass and heat transfer, fluid dynamics, thermomechanics etc.)
- Topic of diploma thesis: Particle deposition in human respiratory airways

Work Experience:

08/2012 – present Faculty of Mechanical Engineering, BUT

Young Researcher

- Study of the flow field in the human respiratory tract
- The use of various visualization techniques, such as highspeed camera, and optical methods (PIV, LDA)
- Analysis of the measured flow fields, calculation of velocities and turbulence characteristics (software Tecplot, Origin), comparison of the results with the computational fluid dynamics results (CFD)
- Matlab programming
- Various aerosol measurements (particle size distribution, concentration, density), dilution, measurement of filtration efficiency
- Design and assemble of experimental setups for the flow measurements

Other Trainings:

2012/2013 Research fellowship at Clarkson University, Potsdam, USA (3 months)

- Study of fibrous particle transport in channels. Measurements of fiber deposition in the human respiratory tract model.

2013/2014 Research fellowship at École Centrale Marseille, France (3 weeks)

- The use of particle image velocimetry for the flow measurement (PIV).

2014/2015 Work internship at Phillip Morris International, Neuchatel, Switzerland (3 months)

- Electronic cigarrete smoke analysis (particle size measurements, concentration). Deposition measurements of multi-component aerosol in the human respiratory tract model.

Projects:

2012–2017 Projects funded by the Ministry of education, youth and sports and Czech grant agency (member of the research group)

- Deposition of radioactive particles in the human respiratory tract model. Analysis of the results using positron emission tomography technique
- Analysis of the flow field using Laser Doppler Velocimetry. Study of the turbulence in the vicinity of vocal cords and airway branching

2014 Junior project funded by the Ministry of education, youth and sports (principal investigator)

- Generation of porous particles
- The effect of porosity on particle transport. Deposition measurements of porous particles in the human respiratory tract

Other skills:

Native language:	Czech	
Other languages:	English:	Cambridge English Certificate: Advanced (CAE)
	German:	basic
Computer skills:	MS Office	

Driving license: B – active driver

Abstract

Inhalation of airborne particulate matter can trigger or exacerbate pre–existing lung conditions. On the other hand, inhalation of aerosolized medicaments can be used for treatment of various respiratory or systemic diseases. In both cases, it is essential to comprehend the particle transport and subsequent deposition. The aim of this PhD thesis is to obtain new experimental data on particle deposition and elucidate the effect of particle shape and flow rate on deposition.

The deposition of porous and fibrous particles in the realistic replica of human respiratory airways was studied. The porous particles were produced by various methods, such as spray–drying or liquid–liquid interface crystallization. The produced particles were introduced into the replica and the subsequent deposition was detected using spectrophotometry. The fibrous particles were produced by crushing glass wool material. To narrow the fiber size distribution, the resulting fibers were sieved and then classified according to their length using a dielectrophoretic classifier. The fiber deposition inside the replica was detected using phase–contrast microscopy. To speed–up this analysis, an in–house software based on image processing was developed.

The results were utilized to calculate deposition characteristics. The deposition efficiency of both particle types increased with increasing Stokes number indicating a significant role of impaction. Comparing their deposition efficiency to that of spherical particles, porous particles exhibited similar deposition efficiencies, however, fibers deposited less efficiently than spherical particles having the same Stokes number. As the boundary conditions were sufficiently described and the replica is available in a digital format, the data can be also employed in validation of numerical simulations.